Immunoblot analysis was performed as described previously (Hidajat *et al.*, 2005). Mouse mAbs against Myc (9E10), NS3, NS4A (S4-13; a kind gift from Dr I. Fuke) and p53 (Ab-1; Calbiochem) were used as primary antibodies and peroxidase-labelled goat anti-mouse IgG (MBL) as a secondary antibody. The protein bands were visualized by an enhanced chemiluminescence method (ECL; Amersham Biosciences) and the intensity of the bands was quantified by using NIH Image 1.61.

Luciferase reporter assay. p53-Luc (Stratagene), which contains the *Photinus pyralis* (firefly) luciferase reporter gene driven by a basic promoter element plus an inducible *cis*-enhancer element, containing 14 repeats of the p53-binding sequence (TGCCTGGACTTGCCTGG), was used as a reporter plasmid. pRL-SV40 (Promega), which expresses *Renilla* luciferase, was used as a control plasmid to check transfection efficiency. Huh-7 cells prepared in a 24-well tissue-culture plate were transfected transiently with p53-Luc (10 ng), pRL-SV40 (1 ng), pSG5/p53 (5 ng) and pSG5/NS3-N or pSG5/NS3-Full (250 ng) in the absence or presence of pSG5/NS4A (75 ng). After 24 h, the cells were harvested and a luciferase assay was performed by using the Dual-Luciferase Reporter Assay system (Promega), as described previously (Kadoya *et al.*, 2005). Firefly and *Renilla* luciferase activities were measured by using a Luminescencer-JNR AB-2100 (Atto). Firefly luciferase activity was normalized to *Renilla* luciferase activity for each sample.

NS3 serine protease activity. HeLa cells transiently coexpressing NS5A/5BΔC and Myc-tagged NS3 were lysed in gel-loading buffer containing 50 mM Tris/HCl (pH 6·8), 5 % 2-mercaptoethanol, 2 % SDS, 0·1 % bromophenol blue and 10 % glycerol. The lysates were separated by SDS-PAGE and analysed by immunoblotting using anti-NS5A (8926; a kind gift from Dr I. Fuke) and anti-Myc antibodies (9E10). Intensity of the bands corresponding to the cleaved NS5A and the uncleaved NS5A/5BΔC was measured. Arbitrary units of serine protease activity of each NS3 were calculated by the following formula: protease activity (arbitrary units) = NS5A/(NS5A/5BΔC + NS5A).

RESULTS

NS3-N sequences of different HCV-1b isolates exhibit distinct subcellular-localization patterns in a sequence-dependent manner

We first examined the subcellular localization of NS3-N in HeLa cells. As shown in Fig. 1(a), we noticed three distinct patterns of NS3-N localization: (i) dot-like staining in both the cytoplasm and the nucleus, (ii) diffuse staining predominantly in the cytoplasm and (iii) a mixed pattern of the former two. Of the 29 HCV-1b isolates tested, 15 (52 %) exhibited exclusively the dot-like staining, nine (31 %) the diffuse staining and the remaining five (17 %) the mixed pattern. The subcellular-localization patterns of four NS3-N sequences each from the dot-like, diffuse and mixed staining groups are also shown in Supplementary Fig. S1 (available in JGV Online). Similar results were obtained when NS3-N sequences were expressed in Huh-7 cells (data not shown), suggesting that the distinct localization patterns among different NS3 sequences are not restricted to a particular cell line.

In order to see which amino acid residue(s) affected the subcellular localization of NS3, we determined the sequences of all 29 isolates. Some of the sequences showing the typical localization patterns, along with a standard sequence, are shown in Fig. 1(b). For more information, the sequences of all 29 isolates are shown in Supplementary Fig. S2 (available in JGV Online). We did not find any common amino acid residue(s) that was/were associated with a particular localization pattern. We noticed, however, that a substitution at position 17 or 18 (Ile to Val) was observed with some NS3 sequences of the dot-like pattern, but not with any NS3 sequences of the other localization patterns. Also, a substitution(s) at positions 150–153 (Val to Ala, Ile to Val) appeared to be more frequent in NS3 sequences of the dot-like pattern. To examine the possible importance of those substitutions, we introduced a point mutation(s) to some NS3-N of the dot-like pattern (Fig. 1c). Introduction of two point mutations at positions 18 and 153 into NS3-N of isolate H05-5 did not alter the localization pattern. However, introduction of an additional two point mutations at positions 80 and 122 altered the localization pattern significantly, with the majority of the cells exhibiting the typical diffuse staining. Similarly, introduction of two mutations at positions 17 and 86, but not of either one alone, into NS3-N of isolate 45 altered the localization pattern from dot-like to diffuse staining. As for isolate 63, a single point mutation at position 150 alone was enough to change the localization pattern of NS3-N. These results suggest that residues at positions 17 or 18, 80–86 and/or 150–153 play an important role in determining the localization pattern of some, but not all, NS3 sequences.

NS3-N binds to p53 and inhibits its *trans*-activating activity in an NS3 sequence-dependent manner

We previously reported that a region near the N terminus of NS3 (aa 29–174) was involved in complex formation with p53 (Ishido & Hotta, 1998). In this study, we examined whether interaction between NS3-N and p53 differs with different NS3-N sequences. We selected two NS3-N sequences each from the dot-like (H05-5 and 45) and diffuse (H17-2 and 42) staining groups. Co-immunoprecipitation analysis demonstrated that NS3-N of isolate H05-5 interacted with p53 most strongly, followed by that of isolate 45, both in the absence (Fig. 2a) and the presence (Fig. 2b) of NS4A. On the other hand, NS3-N of the diffuse-staining group interacted only weakly with p53. The specificity of the interaction between NS3-N and p53 was confirmed by a control experiment, in which neither NS4A nor NS4B bound to p53 under the same experimental conditions (Fig. 2c, left and centre panels). The specificity of the NS3–p53 interaction was also secured by another control experiment using an irrelevant (anti-FLAG) antibody (Fig. 2c, right panel).

Next, we examined the possible effect of NS3-N on p53 function. The plasmid p53-Luc harbours 14 copies of p53-responsive elements and a minimum promoter upstream of a luciferase gene, and is used to monitor p53-dependent transcriptional activity. Interestingly, NS3-N of H05-5 and that of isolate 45 inhibited p53-dependent transcription of the luciferase gene strongly and moderately, respectively

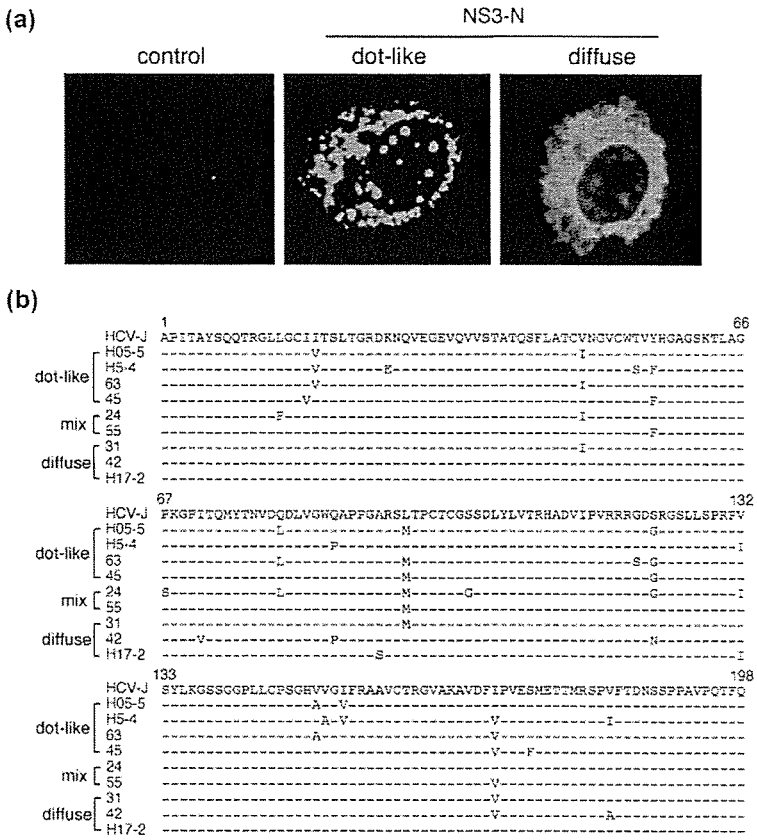

Fig. 1. Distinct subcellular-localization patterns of NS3-N of different HCV-1b isolates and the alignment of their sequences. (a) NS3-N was expressed in HeLa cells using a vaccinia virus–T7 hybrid expression method. Typical immunofluorescence images of the dot-like (middle panel) and diffuse (right panel) localization patterns of NS3-N of isolates H05-5 and H17-2, respectively, are shown. As a control, cells expressing NS3-N of H05-5 (left panel) were stained with an irrelevant (anti-HA) antibody. (b) Sequence alignment of representative sequences of each of the staining groups along with a standard sequence of the HCV-J strain (top). Dashes indicate residues identical to those of HCV-J. The numbers along the sequence indicate amino acid positions. (c) Identification of residues that alter the localization patterns of NS3-N of the isolates H05-5, 45 and 63. Substituted residues at the indicated positions are shown.

(Fig. 2d). On the other hand, no inhibition was observed with NS3-N of isolate 42 and even a slight increase in p53-dependent transcription was observed with NS3-N of H17-2.

NS3 forms a stable complex with its cofactor NS4A, which may counteract the NS3-mediated inhibitory action of p53-dependent transcription. In fact, we observed that inhibition of the p53-dependent transcription by NS3-N of the H05-5 isolate was alleviated to some extent, but not completely, by coexpression of NS4A (Fig. 2e).

To further test the possibility that the alteration in the localization pattern of NS3-N affects its interaction with p53, we compared NS3-N of H05-5 with its point mutant H05-5/mut (Fig. 1c) in terms of their p53-binding abilities and inhibitory effects on p53-dependent transcription. The result obtained demonstrated that NS3-N of H05-5/mut, which showed diffuse localization, had weaker p53-binding capacity (Fig. 3a) and exerted weaker inhibition on p53-dependent transcription (Fig. 3b) compared with NS3-N of the parental H05-5, showing the dot-like localization. Similar results were obtained with isolates 45 and 63 and their point mutants (data not shown). Our results thus suggest that NS3-N of the dot-like localization pattern interacts with p53 more strongly and inhibits p53-mediated transcriptional activation more efficiently than that of the diffuse localization.

NS3-Full sequences exhibit the same subcellular-localization patterns as those of NS3-N sequences derived from the same isolates and interact differentially with NS4A and p53 in an NS3 sequence-dependent manner

As shown above, NS3-N exhibited a distinct subcellular-localization pattern in a sequence-dependent manner when expressed alone (see Fig. 1). Moreover, we have reported that NS3, either NS3-N or NS3-Full, enters the nucleus when

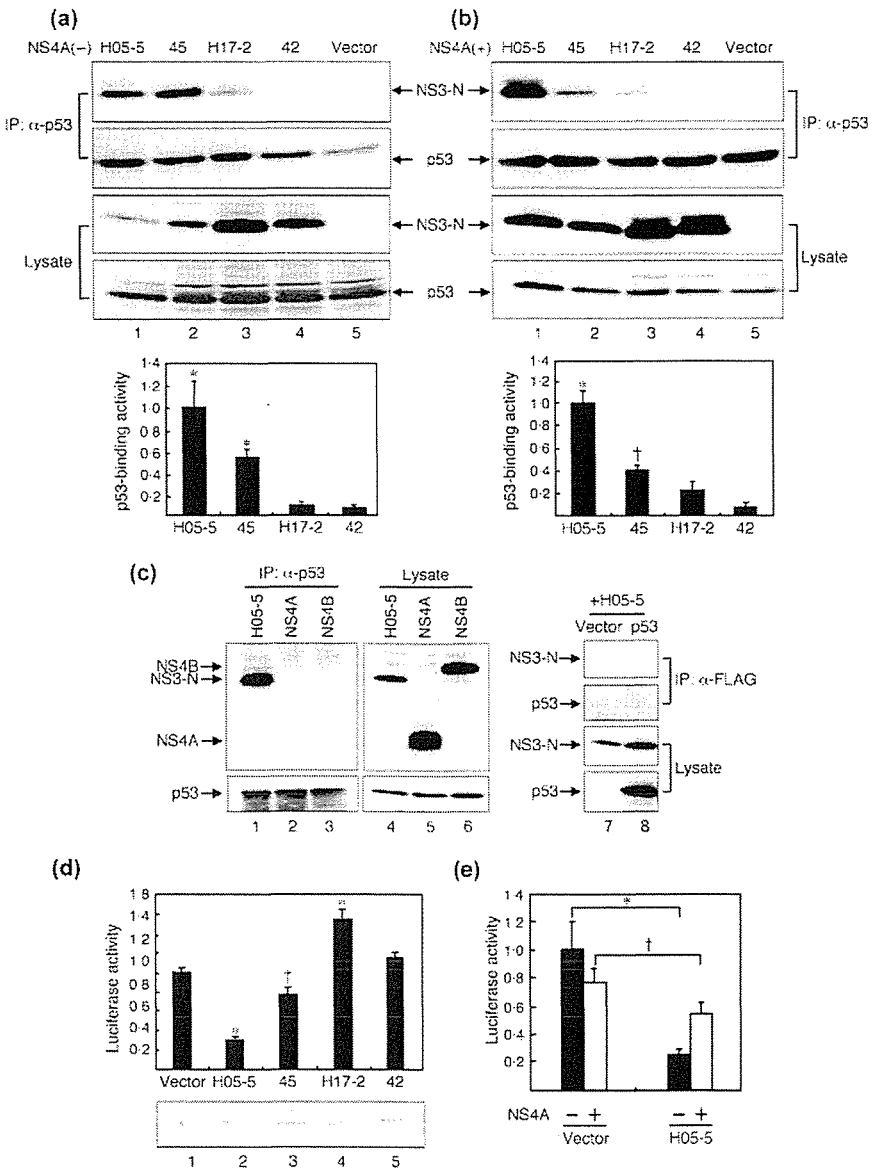

Fig. 2. Physical and functional interactions between NS3-N and p53 in an NS3 sequence-dependent manner. NS3-N and p53 were coexpressed in the absence (a) and presence (b) of NS4A. Cells that did not express NS3-N served as a control. Cell lysates were immunoprecipitated by using an anti-p53 antibody and probed by immunoblotting using an anti-Myc antibody to detect NS3-N (top row). Efficient immunoprecipitation of p53 was verified (second row). Lysates were probed directly (without being immunoprecipitated with anti-p53 antibody) with anti-Myc and anti-p53 antibodies, respectively, to verify comparable expression levels of NS3-N (third row) and p53 (bottom row). The intensity of the bands for NS3-N co-immunoprecipitated with p53 was quantified and normalized to the expression levels of NS3-N in the lysates. Filled columns and bars represent mean ± SD obtained from three independent experiments. The p53-binding intensity of NS3-N of the isolate H05-5 was expressed as 1·0. $^*P<0{\cdot}01$; $\dagger P<0{\cdot}05$, compared with isolate 42. (c) Cells expressing Myc-tagged H05-5, NS4A or NS4B together with p53 were analysed by immunoprecipitation using an anti-p53 antibody (left). Lysates were probed directly with anti-Myc and anti-p53 antibodies, respectively (middle). Cells expressing Myc-tagged H05-5 with or without p53 were analysed by immunoprecipitation using an irrelevant (anti-FLAG) antibody (right). (d) Inhibition of p53-dependent transcription by NS3-N in an NS3 sequence-dependent manner. pSG5-based NS3-N expression plasmids were each co-transfected with pSG5/p53, p53-Luc and pRL-SV40 in Huh-7 cells and cultivated for 24 h. Firefly luciferase activity was measured and normalized to *Renilla* luciferase activity. The luciferase activity in the control cells without NS3-N expression was expressed arbitrarily as 1·0. Results are shown as mean ± SD from three independent experiments. $^*P<0{\cdot}01$; $\dagger P<0{\cdot}05$, compared with the control. Expression levels of NS3-N in the cells are shown at the bottom. (e) Inhibition of p53-dependent transcription by NS3-N of H05-5 in the absence (filled bars) and presence (open bars) of NS4A. Results are shown as mean ± SD from three independent experiments. $^*P<0{\cdot}01$; $\dagger P<0{\cdot}05$, compared with the control.

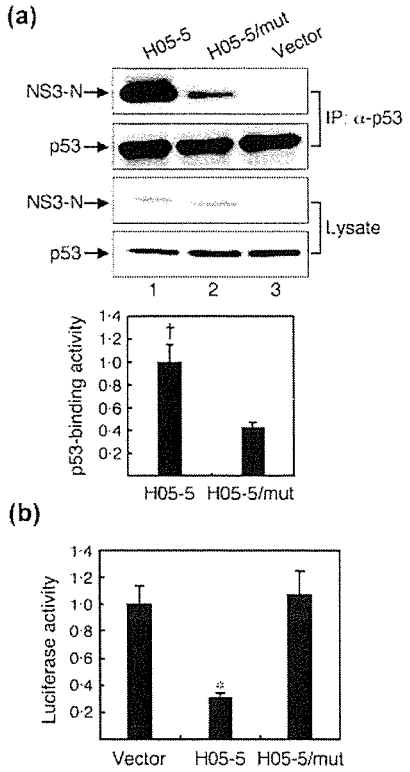

Fig. 3. Comparison between NS3-N of the isolate H05-5 and its point mutant H05-5/mut in their capacity to interact with p53. (a) Physical interaction with p53 was analysed as described in the legend to Fig. 2(a). Filled columns and bars represent mean ± SD obtained from three independent experiments. The p53-binding intensity of NS3-N of H05-5 was expressed as 1·0. †$P<0·05$. (b) Functional interaction with p53 was analysed as described in the legend to Fig. 2(c). Results are shown as mean ± SD from three independent experiments. *$P<0·01$ compared with H05-5/mut.

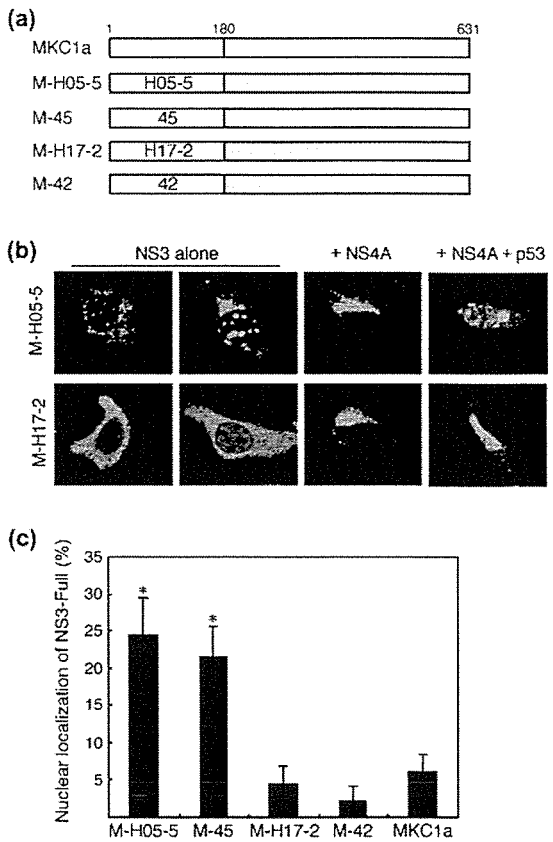

Fig. 4. Subcellular localization of NS3-Full in the presence and absence of NS4A and p53. (a) Schematic representation of NS3-Full of different sequences. The N-terminal 180 residues are derived from clinical isolates (H05-5, H17-2, 42 and 45) and the C-terminal 451 residues from the parental MKC1a strain. (b) Subcellular localization of M-H05-5 (upper) and M-H17-2 (lower) when expressed alone, when coexpressed with NS4A and when coexpressed with NS4A and p53. The cells were stained with either anti-NS3 (left panels) or anti-Myc antibody (left-middle, right-middle and right panels). (c) Percentage of cells with nuclear accumulation of NS3-Full when coexpressed with NS4A and p53. *$P<0·01$ compared with M-42.

coexpressed with p53 and that the p53-mediated nuclear localization of NS3 is inhibited by NS4A in an NS3 sequence-dependent manner (Muramatsu *et al.*, 1997). Therefore, we examined the subcellular-localization patterns of NS3-Full of different sequences, both when expressed alone and when coexpressed with p53 and/or NS4A. The NS3-Full sequences tested differ from each other only in the N-terminal 180 residues that are derived from the clinical isolates, with the C-terminal 451 residues being shared among all the strains tested (Fig. 4a; Hidajat *et al.*, 2005). When expressed alone, NS3-Full of all four strains exhibited the same subcellular-localization patterns as those of NS3-N of the same strains (Fig. 4b; data not shown for M-45 and M-42). When coexpressed with NS4A, NS3-Full was localized in the cytoplasm, especially in perinuclear regions, regardless of the strain tested. Interestingly, when p53 was additionally coexpressed with NS4A, NS3-Full of the dot-like type (M-H05-5 and M-45) showed an increased tendency to accumulate in the nucleus together with p53 (Fig. 4b), with nearly 25 % of the cells exhibiting nuclear localization of NS3 (Fig. 4c). Concomitant expression of NS4A in the cytoplasm of the same cells was confirmed by double-staining immunofluorescence analysis (data not shown), the result being consistent with our previous observation (Ishido *et al.*, 1997). On the other hand, NS3-Full of the diffuse type (M-H17-2, M-42 and MKC1a) was localized almost exclusively in the cytoplasm together with NS4A. Similar results were obtained when NS3-N sequences of different isolates were coexpressed with p53 and/or NS4A (data not shown).

We then tested complex formation between NS3-Full of the five different sequences and p53. The results demonstrated clearly that NS3-Full of the dot-like type (M-H05-5 and

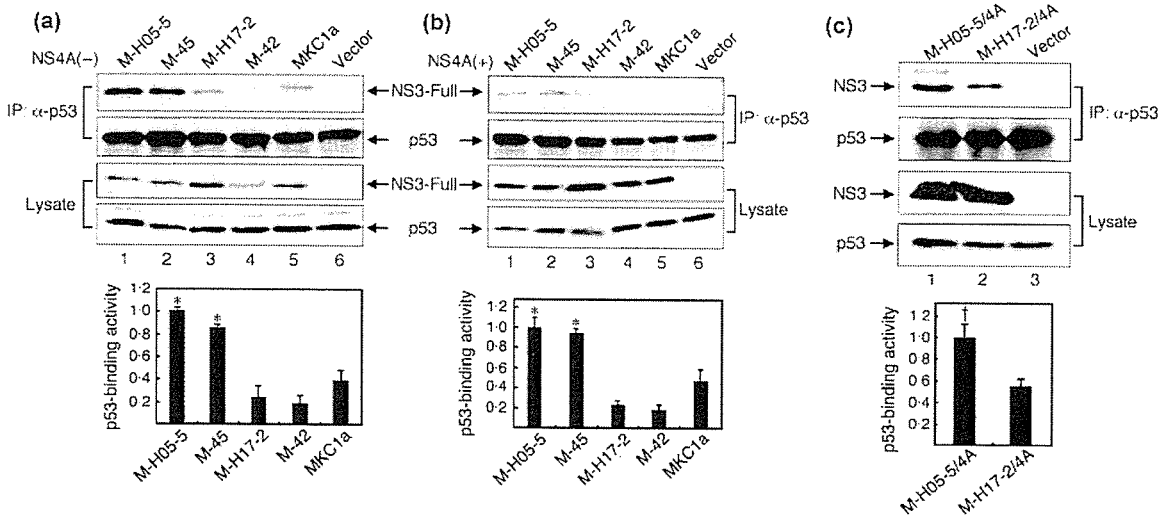

Fig. 5. Physical interaction between NS3-Full and p53 in an NS3 sequence-dependent manner. NS3-Full of different strains in the absence (a) and presence of NS4A coexpression *in trans* (b) were analysed as described in the legend to Fig. 2(a). Filled columns and bars represent mean ± SD obtained from three independent experiments. The p53-binding intensity of M-H05-5 was expressed as 1·0. *$P<0·01$ compared with M-42. (c) M-H05-5/4A and M-H17-2/4A (NS3–4A coexpression *in cis*) were analysed as described in the legend to Fig. 2(a), except that anti-NS3 antibody was used instead of anti-Myc antibody. Filled columns and bars represent mean ± SD obtained from three independent experiments. The p53-binding intensity of M-H05-5/4A was expressed as 1·0. †$P<0·05$ compared with M-H17-2/4A.

M-45) interacted with p53 more strongly than that of the diffuse type (M-H17-2, M-42 and MKC1a), both in the absence and presence of NS4A (Fig. 5a, b). In this connection, it should be noted that the interaction between NS3-Full and p53 was weaker in the presence of NS4A than in its absence. We also examined the interaction of NS3 with p53 when full-length NS3–4A was expressed *in cis*, where NS3–4A complex formation occurs more efficiently than *in trans*. The results demonstrated that M-H05-5/4A interacted with p53 more strongly than did M-H17-2/4A (Fig. 5c), again suggesting NS3 sequence-dependent interaction with p53.

NS3 binds to p53 and inhibits its *trans*-activating activity in HCV RNA replicon-harbouring cells

In order to determine whether NS3 expressed in the context of HCV replication interacted with p53, we used Huh-7 cells harbouring an HCV subgenomic RNA replicon and examined physical and functional interactions between NS3 and p53. Co-immunoprecipitation analysis revealed that NS3 interacted physically with p53 in HCV subgenomic RNA replicon-harbouring cells, albeit with much lower efficiency than in the plasmid-based expression system (Fig. 6a). We also used the full-length HCV RNA replicon, whose NS3 is detected more strongly than that of the subgenomic RNA replicon by the anti-NS3 mAb used in this study. The result demonstrated that NS3 expressed in the context of HCV RNA replication interacted efficiently with p53, irrespective of whether p53 was expressed ectopically or endogenously (Fig. 6b). The specificity of the interaction between NS3 and p53 was confirmed by the lack of interaction between NS4A and p53 in HCV subgenomic RNA-harbouring cells (Fig. 6c). Next, we compared *trans*-activating activity of p53 between HCV RNA replicon-harbouring cells and the HCV-negative controls (parental and cured Huh-7 cells). We observed that p53-dependent transcription was suppressed significantly in cells harbouring an HCV RNA replicon, either subgenomic or full-length, compared with the parental and cured Huh-7 cells (Fig. 6d, e). These results suggest collectively that NS3 expressed in the context of HCV replication inhibits p53 function.

Serine protease activity of NS3-Full in the absence and presence of NS4A

The N-terminal portion of NS3 possesses a serine protease activity that can cleave the NS5A/5B junction even in the absence of NS4A (Lin *et al.*, 1994). By using NS5A/5BΔC as a substrate, we compared the serine protease activities of NS3-Full of different subcellular-localization patterns. A tendency was noted that, in the absence of NS4A, NS3-Full of the dot-like type showed slightly weaker protease activity than that of the diffuse type (Fig. 7). This difference might be attributable, at least partly, to the fact that NS5A/5BΔC was localized diffusely in the cytoplasm (Kim *et al.*, 1999; Mottola *et al.*, 2002; data not shown) and, therefore, could be recognized more easily by NS3 of the same localization pattern than by NS3 of the other type. In the presence of

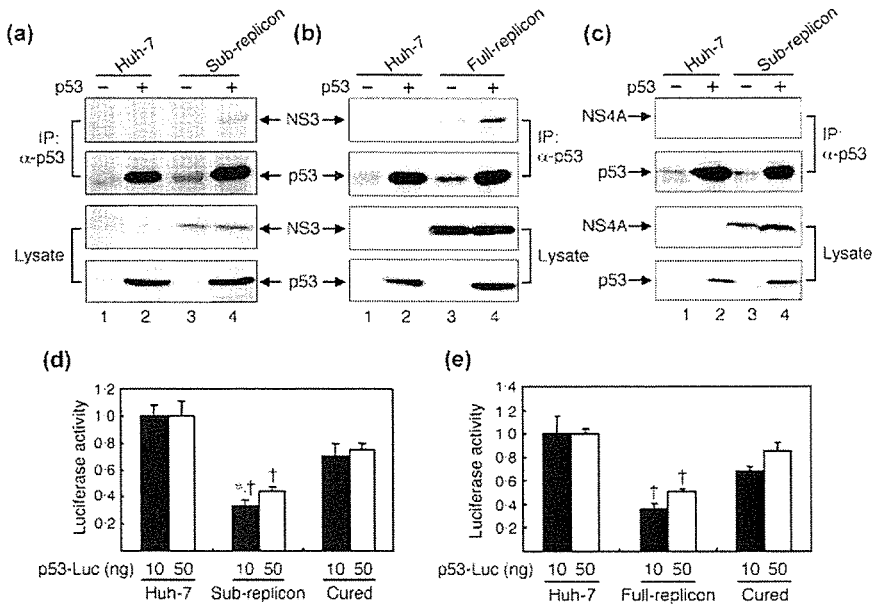

Fig. 6. Physical and functional interactions between NS3 and p53 in HCV RNA replicon-harbouring cells. p53 was expressed ectopically in Huh-7 cells harbouring either HCV subgenomic (a) or full-length (b) RNA replicon and the parental Huh-7 cells by using a vaccinia virus–T7 hybrid expression method. Cell lysates were analysed as described in Methods. (c) The lack of interaction between NS4A and p53 in HCV subgenomic RNA replicon-harbouring Huh-7 cells was confirmed. Inhibition of p53-dependent transcription in Huh-7 cells harbouring either HCV subgenomic (d) or full-length (e) RNA replicon. Cells were co-transfected with p53-Luc (10 and 50 ng, filled and open bars, respectively), pSG5/p53 (10 ng) and pRL-SV40 (1 ng) as an internal control. After 24 h, firefly luciferase activity was measured and normalized to *Renilla* luciferase activity. Luciferase activities in the parental Huh-7 cells were expressed arbitrarily as 1·0. Cured cells also served as a control. Results are shown as mean ± SD from three independent experiments. $*P<0·01$; $\dagger P<0·05$, compared with the parental and cured Huh-7 cells.

NS4A, on the other hand, all of the NS3-Full sequences, which accumulated at a perinuclear region of the cytoplasm (see Fig. 4b), exhibited an enhanced and comparable degree of serine protease activity among the five strains (Fig. 7). Similar results were obtained when Huh-7 cells were used instead of HeLa cells (data not shown).

DISCUSSION

In the present study we demonstrated that, when expressed alone, NS3 of HCV-1b isolates, either NS3-N or NS3-Full, exhibited distinct subcellular-localization patterns, i.e. (i) dot-like staining both in the cytoplasm and the nucleus, (ii) diffuse staining predominantly in the cytoplasm and (iii) a mixed type, in a sequence-dependent manner (Figs 1 and 4). Although no significant correlation has been observed so far between the localization patterns of NS3 and the HCC status of the patients, it was interesting to find that NS3-N and NS3-Full of the dot-like staining pattern interacted with p53 more strongly than that of the diffuse-staining pattern (Figs 2a, 3a and 5a). Similar results were obtained when NS3 was coexpressed with NS4A (Figs 2b, 5b and 5c). We also observed that both NS3-N and NS3-Full of the dot-like staining pattern, but not those of the diffuse pattern, were more prone to colocalize with p53 in the nucleus even in the presence of NS4A (Fig. 4). Luciferase reporter analysis demonstrated that NS3-N of the dot-like type, but not that of the diffuse type, suppressed p53-dependent transcriptional activation significantly (Figs 2d and 3b).

When cells are exposed to a variety of stresses, p53 is induced to accumulate in the nucleus, where it functions as a transcription factor for cell-cycle regulators such as p21 (Levine, 1997). Our present results demonstrated that NS3-N of isolate H05-5 inhibited p53-dependent transcription of a reporter gene strongly (Figs 2d and 3b). We need to assess two possible mechanisms for the NS3-N-mediated p53 inhibition: NS3 might inhibit either p53 expression or p53 function itself. Our results showed that p53 expression levels were not altered significantly by NS3-N, irrespective of the localization patterns (Fig. 2a, b, bottom). Similar results that neither p53 mRNA nor protein levels were downregulated by NS3 were reported by Kwun *et al.* (2001). Overexpression of p53 was even observed in hepatocytes of some, if not all, HCV-infected patients (Loguercio *et al.*, 2003). It is likely, therefore, that NS3-N inhibits p53 function by interacting with it physically.

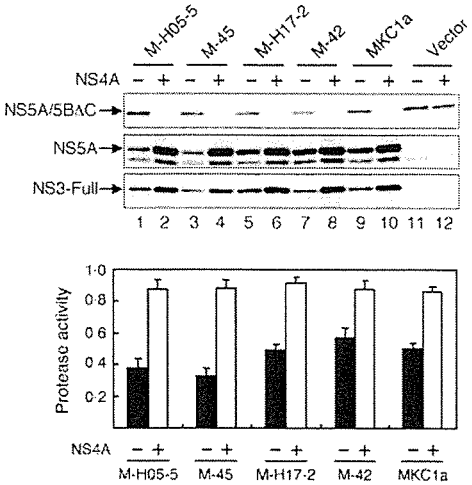

Fig. 7. Serine protease activity of NS3-Full in the absence and presence of NS4A. NS3-Full of different strains and NS5A/5BΔC were coexpressed in HeLa cells without (lanes with odd numbers) or with (lanes with even numbers) NS4A using a vaccinia virus–T7 hybrid expression method. Cell lysates were subjected to immunoblotting using anti-NS5A or anti-Myc antibody to detect NS5A/5BΔC (top), NS5A (middle) and NS3 (bottom). The intensity of the bands was quantified and arbitrary units of serine protease activity were calculated as described in Methods. Serine protease activities of NS3-Full in the absence (filled bars) and presence (open bars) of NS4A obtained from three independent experiments are shown.

We previously reported that a region of p53 near the C terminus (aa 301–360) was involved in complex formation with NS3 (Ishido & Hotta, 1998). This region includes the p53 oligomerization domain (aa 324–355) (Levine, 1997). It is known that the p53 tetramer binds to the p53-response element on promoter sequences most efficiently and, therefore, is most effective in *trans*-activation of its target genes (McLure & Lee, 1998; Weinberg *et al.*, 2004). Recently, it was reported that proteins of the S100 family disrupted p53 tetramerization via binding to its tetramerization domain (Fernandez-Fernandez *et al.*, 2005). Therefore, it is reasonable to assume that interaction of NS3-N with p53 interferes with its tetramer formation and DNA binding, thereby inhibiting p53-dependent transcriptional activation. It was also reported that a C-terminal portion of p53 (aa 364–393) negatively regulated its DNA-binding capacity (Müller-Tiemann *et al.*, 1998) and that the 14-3-3 proteins could associate with this region to counteract the negative regulation, which resulted in increased DNA binding of p53 (Waterman *et al.*, 1998). It is tempting to speculate that, by binding to a nearby region of p53, NS3-N may impair the association of 14-3-3 proteins with p53, which results in comparably decreased DNA binding of p53. Moreover, p53 is subject to post-translational modifications, including phosphorylation and acetylation, that affect p53 function (Appella & Anderson, 2001). Further study is needed to determine whether such p53 modification status is affected, either directly or indirectly, by NS3-N.

Consistent with the results obtained from transient-expression experiments, physical interaction between NS3 and p53 was also observed in Huh-7 cells harbouring either an HCV subgenomic or full-length RNA replicon, albeit to a smaller extent than in the transient-expression system (Fig. 6). It should be noted that NS3 expressed by the full-length RNA replicon is detected more strongly by the anti-NS3 antibody used in this study than that of the subgenomic RNA replicon. In HCV RNA replicon-harbouring cells, the HCV non-structural proteins are incorporated into the HCV RNA replication complex and, therefore, it is conceivable that only a minor fraction of NS3 is available for the interaction with p53. Nevertheless, p53-mediated transcriptional activation was suppressed significantly in HCV RNA replicon-harbouring cells compared with the controls (Fig. 6d, e). We must consider the possibility that not only NS3, but also other HCV proteins, are involved in the observed p53 inhibition. In fact, interaction between NS5A and p53 has been reported (Lan *et al.*, 2002; Qadri *et al.*, 2002).

In conclusion, our present results have demonstrated that NS3 of HCV-1b can be divided into three groups based on the subcellular-localization patterns and that NS3 of the dot-like localization pattern interacts with, and inhibits the function of, the tumour suppressor p53 more strongly than that of the diffuse type. The observed difference may account, at least partly, for a different degree of the oncogenic capacity of different HCV-1b isolates.

ACKNOWLEDGEMENTS

The authors are grateful to Dr I. Fuke, Research Institute for Microbial Diseases, Kan-Onji Branch, Kagawa, Japan, for providing anti-NS3, anti-NS4A and anti-NS5A mAbs. Thanks are also due to Dr R. Bartenschlager (University of Heidelberg, Heidelberg, Germany) for providing an HCV subgenomic RNA replicon (pFK5B/2884Gly). This study was supported in part by Grants-in-Aid for Scientific Research from the Ministry of Education, Culture, Sports, Science and Technology, the Japan Society for the Promotion of Science and the Ministry of Health, Labour and Welfare, Japan. This study was also carried out as part of the 21COE Program at Kobe University Graduate School of Medicine.

REFERENCES

Appella, E. & Anderson, C. W. (2001). Post-translational modifications and activation of p53 by genotoxic stresses. *Eur J Biochem* **268**, 2764–2772.

Breiman, A., Grandvaux, N., Lin, R., Ottone, C., Akira, S., Yoneyama, M., Fujita, T., Hiscott, J. & Meurs, E. F. (2005). Inhibition of RIG-I-dependent signaling to the interferon pathway during hepatitis C virus expression and restoration of signaling by IKKε. *J Virol* **79**, 3969–3978.

Cheng, P.-L., Chang, M.-H., Chao, C.-H. & Wu Lee, Y.-H. (2004). Hepatitis C viral proteins interact with Smad3 and differentially regulate TGF-β/Smad3-mediated transcriptional activation. *Oncogene* **23**, 7821–7838.

Fernandez-Fernandez, M. R., Veprintsev, D. B. & Fersht, A. R. (2005). Proteins of the S100 family regulate the oligomerization of p53 tumor suppressor. *Proc Natl Acad Sci U S A* **102**, 4735–4740.

Florese, R. H., Nagano-Fujii, M., Iwanaga, Y., Hidajat, R. & Hotta, H. (2002). Inhibition of protein synthesis by the nonstructural proteins NS4A and NS4B of hepatitis C virus. *Virus Res* **90**, 119–131.

Foy, E., Li, K., Wang, C., Sumpter, R., Jr, Ikeda, M., Lemon, S. M. & Gale, M., Jr (2003). Regulation of interferon regulatory factor-3 by the hepatitis C virus serine protease. *Science* **300**, 1145–1148.

Foy, E., Li, K., Sumpter, R., Jr & 8 other authors (2005). Control of antiviral defenses through hepatitis C virus disruption of retinoic acid-inducible gene-I signaling. *Proc Natl Acad Sci U S A* **102**, 2986–2991.

Fuerst, T. R., Niles, E. G., Studier, F. W. & Moss, B. (1986). Eukaryotic transient-expression system based on recombinant vaccinia virus that synthesizes bacteriophage T7 RNA polymerase. *Proc Natl Acad Sci U S A* **83**, 8122–8126.

Fujita, T., Ishido, S., Muramatsu, S., Itoh, M. & Hotta, H. (1996). Suppression of actinomycin D-induced apoptosis by the NS3 protein of hepatitis C virus. *Biochem Biophys Res Commun* **229**, 825–831.

Hidajat, R., Nagano-Fujii, M., Deng, L., Tanaka, M., Takigawa, Y., Kitazawa, S. & Hotta, H. (2005). Hepatitis C virus NS3 protein interacts with ELKS-δ and ELKS-α, members of a novel protein family involved in intracellular transport and secretory pathways. *J Gen Virol* **86**, 2197–2208.

Ikeda, M., Abe, K., Dansako, H., Nakamura, T., Naka, K. & Kato, N. (2005). Efficient replication of a full-length hepatitis C virus genome, strain O, in cell culture, and development of a luciferase reporter system. *Biochem Biophys Res Commun* **329**, 1350–1359.

Ishido, S. & Hotta, H. (1998). Complex formation of the non-structural protein 3 of hepatitis C virus with the p53 tumor suppressor. *FEBS Lett* **438**, 258–262.

Ishido, S., Muramatsu, S., Fujita, T., Iwanaga, Y., Tong, W.-Y., Katayama, Y., Itoh, M. & Hotta, H. (1997). Wild-type, but not mutant-type, p53 enhances nuclear accumulation of the NS3 protein of hepatitis C virus. *Biochem Biophys Res Commun* **230**, 431–436.

Kadoya, H., Nagano-Fujii, M., Deng, L., Nakazono, N. & Hotta, H. (2005). Nonstructural proteins 4A and 4B of hepatitis C virus transactivate the interleukin 8 promoter. *Microbiol Immunol* **49**, 265–273.

Kao, C.-F., Chen, S.-Y., Chen, J.-Y. & Wu Lee, Y.-H. (2004). Modulation of p53 transcription regulatory activity and post-translational modification by hepatitis C virus core protein. *Oncogene* **23**, 2472–2483.

Kim, D. W., Gwack, Y., Han, J. H. & Choe, J. (1995). C-terminal domain of the hepatitis C virus NS3 protein contains an RNA helicase activity. *Biochem Biophys Res Commun* **215**, 160–166.

Kim, J.-E., Song, W. K., Chung, K. M., Back, S. H. & Jang, S. K. (1999). Subcellular localization of hepatitis C viral proteins in mammalian cells. *Arch Virol* **144**, 329–343.

Kwun, H. J., Jung, E. Y., Ahn, J. Y., Lee, M. N. & Jang, K. L. (2001). p53-dependent transcriptional repression of $p21^{waf1}$ by hepatitis C virus NS3. *J Gen Virol* **82**, 2235–2241.

Lan, K.-H., Sheu, M.-L., Hwang, S.-J. & 8 other authors (2002). HCV NS5A interacts with p53 and inhibits p53-mediated apoptosis. *Oncogene* **21**, 4801–4811.

Levine, A. J. (1997). p53, the cellular gatekeeper for growth and division. *Cell* **88**, 323–331.

Lin, C., Prágai, B. M., Grakoui, A., Xu, J. & Rice, C. M. (1994). Hepatitis C virus NS3 serine proteinase: *trans*-cleavage requirements and processing kinetics. *J Virol* **68**, 8147–8157.

Loguercio, C., Cuomo, A., Tuccillo, C., Gazzerro, P., Cioffi, M., Molinari, A. M. & Del Vecchio Blanco, C. (2003). Liver p53 expression in patients with HCV-related chronic hepatitis. *J Viral Hepat* **10**, 266–270.

Lohmann, V., Körner, F., Dobierzewska, A. & Bartenschlager, R. (2001). Mutations in hepatitis C virus RNAs conferring cell culture adaptation. *J Virol* **75**, 1437–1449.

Longworth, M. S. & Laimins, L. A. (2004). Pathogenesis of human papillomaviruses in differentiating epithelia. *Microbiol Mol Biol Rev* **68**, 362–372.

Martin, M. E. D. & Berk, A. J. (1998). Adenovirus E1B 55K represses p53 activation in vitro. *J Virol* **72**, 3146–3154.

McLure, K. G. & Lee, P. W. K. (1998). How p53 binds DNA as a tetramer. *EMBO J* **17**, 3342–3350.

Moss, B., Elroy-Stein, O., Mizukami, T., Alexander, W. A. & Fuerst, T. R. (1990). New mammalian expression vectors. *Nature* **348**, 91–92.

Mottola, G., Cardinali, G., Ceccacci, A., Trozzi, C., Bartholomew, L., Torrisi, M. R., Pedrazzini, E., Bonatti, S. & Migliaccio, G. (2002). Hepatitis C virus nonstructural proteins are localized in a modified endoplasmic reticulum of cells expressing viral subgenomic replicons. *Virology* **293**, 31–43.

Müller-Tiemann, B. F., Halazonetis, T. D. & Elting, J. J. (1998). Identification of an additional negative regulatory region for p53 sequence-specific DNA binding. *Proc Natl Acad Sci U S A* **95**, 6079–6084.

Münger, K. & Howley, P. M. (2002). Human papillomavirus immortalization and transformation functions. *Virus Res* **89**, 213–228.

Muramatsu, S., Ishido, S., Fujita, T., Itoh, M. & Hotta, H. (1997). Nuclear localization of the NS3 protein of hepatitis C virus and factors affecting the localization. *J Virol* **71**, 4954–4961.

Ogata, S., Ku, Y., Yoon, S., Makino, S., Nagano-Fujii, M. & Hotta, H. (2002). Correlation between secondary structure of an amino-terminal portion of the nonstructural proteins 3 (NS3) of hepatitis C virus and development of hepatocellular carcinoma. *Microbiol Immunol* **46**, 549–554.

Ogata, S., Florese, R. H., Nagano-Fujii, M. & 7 other authors (2003). Identification of hepatitis C virus (HCV) subtype 1b strains that are highly, or only weakly, associated with hepatocellular carcinoma on the basis of the secondary structure of an amino-terminal portion of the HCV NS3 protein. *J Clin Microbiol* **41**, 2835–2841.

Qadri, I., Iwahashi, M. & Simon, F. (2002). Hepatitis C virus NS5A protein binds TBP and p53, inhibiting their DNA binding and p53 interactions with TBP and ERCC3. *Biochim Biophys Acta* **1592**, 193–204.

Reed, K. E. & Rice, C. M. (2000). Overview of hepatitis C virus genome structure, polyprotein processing, and protein properties. *Curr Top Microbiol Immunol* **242**, 55–84.

Saito, I., Miyamura, T., Ohbayashi, A. & 10 other authors (1990). Hepatitis C virus infection is associated with the development of hepatocellular carcinoma. *Proc Natl Acad Sci U S A* **87**, 6547–6549.

Sakamuro, D., Furukawa, T. & Takegami, T. (1995). Hepatitis C virus nonstructural protein NS3 transforms NIH3T3 cells. *J Virol* **69**, 3893–3896.

Sheppard, H. M., Corneillie, S. I., Espiritu, C., Gatti, A. & Liu, X. (1999). New insights into the mechanism of inhibition of p53 by simian virus 40 large T antigen. *Mol Cell Biol* **19**, 2746–2753.

Taguchi, T., Nagano-Fujii, M., Akutsu, M., Kadoya, H., Ohgimoto, S., Ishido, S. & Hotta, H. (2004). Hepatitis C virus NS5A protein interacts with 2′,5′-oligoadenylate synthetase and inhibits antiviral activity of IFN in an IFN sensitivity-determining region-independent manner. *J Gen Virol* **85**, 959–969.

Tanaka, M., Nagano-Fujii, M., Deng, L., Ishido, S., Sada, K. & Hotta, H. (2006). Single-point mutations of hepatitis C virus NS3 that impair p53 interaction and anti-apoptotic activity of NS3. *Biochem Biophys Res Commun* **340**, 792–799.

Truant, R., Antunovic, J., Greenblatt, J., Prives, C. & Cromlish, J. A. (1995). Direct interaction of the hepatitis B virus HBx protein with p53 leads to inhibition by HBx of p53 response element directed-transactivation. *J Virol* **69**, 1851–1859.

Waterman, M. J. F., Stavridi, E. S., Waterman, J. L. F. & Halazonetis, T. D. (1998). ATM-dependent activation of p53 involves dephosphorylation and association with 14-3-3 proteins. *Nat Genet* **19**, 175–178.

Weinberg, R. L., Veprintsev, D. B. & Fersht, A. R. (2004). Cooperative binding of tetrameric p53 to DNA. *J Mol Biol* **341**, 1145–1159.

Zemel, R., Gerechet, S., Greif, H. & 7 other authors (2001). Cell transformation induced by hepatitis C virus NS3 serine protease. *J Viral Hepat* **8**, 96–102.

Available online at www.sciencedirect.com
SCIENCE DIRECT
ELSEVIER
Virology 346 (2006) 348 – 362
VIROLOGY
www.elsevier.com/locate/yviro

Hepatitis C virus NS5B delays cell cycle progression by inducing interferon-β via Toll-like receptor 3 signaling pathway without replicating viral genomes

Kazuhito Naka [a,1], Hiromichi Dansako [a,1], Naoya Kobayashi [b], Masanori Ikeda [a], Nobuyuki Kato [a,*]

[a] *Department of Molecular Biology, Okayama University Graduate School of Medicine, Dentistry, and Pharmaceutical Sciences, 2-5-1 Shikata-cho, Okayama 700-8558, Japan*
[b] *Department of Surgery, Okayama University Graduate School of Medicine, Dentistry, and Pharmaceutical Sciences, 2-5-1 Shikata-cho, Okayama 700-8558, Japan*

Received 1 July 2005; returned to author for revision 11 August 2005; accepted 18 October 2005
Available online 2 December 2005

Abstract

To clarify the pathogenesis of hepatitis C virus (HCV), we have studied the effects of HCV proteins using human hepatocytes. Here, we found that HCV NS5B, an RNA-dependent RNA polymerase, delayed cell cycle progression through the S phase in PH5CH8 immortalized human hepatocyte cells. Since treatment with anti-interferon (IFN)-β neutralizing antibody restored the cell cycle delay, IFN-β was deemed responsible for the cell cycle delay in NS5B-expressing PH5CH8 cells. The induction of IFN-β and the cell cycle delay were overridden by the down-regulation of Toll-like receptor 3 (TLR3) through RNA interference in NS5B-expressing PH5CH8 cells. Moreover, the NS5B full form was required for the cell cycle delay, the induction of IFN-β, and the activation of the IFN-β signaling pathway. Our findings revealed that NS5B induced IFN-β through the TLR3 signaling pathway in immortalized human hepatocytes even without replicating viral genomes.
© 2005 Elsevier Inc. All rights reserved.

Keywords: Hepatitis C virus; NS5B; Interferon-β; TLR3; Hepatocyte cells

Introduction

Since more than 170 million individuals are estimated to be infected with hepatitis C virus (HCV) worldwide, this disease is a global health problem (Thomas, 2000). HCV belongs to the family Flaviviridae, whose positive-stranded RNA genome encodes a large polyprotein precursor of approximately 3000 amino acid residues. This polyprotein is processed by a combination of the host and viral proteases into at least ten proteins in the following order: NH_2-core-envelope 1-envelope 2-p7-nonstructural protein 2 (NS2)-NS3-NS4A-NS4B-NS5A-NS5B-COOH (Kato, 2001; Kato et al., 1990). These viral proteins are not only involved in viral replication but also may affect a variety of cellular functions (Bartenschlager and Lohmann, 2000; Kato, 2001). Although persistent infection with HCV is a major cause of chronic hepatitis, liver cirrhosis, and hepatocellular carcinoma (HCC) (Colombo, 1996; Kato, 2001), the molecular mechanisms leading to liver cell dysplasia and HCC remain elusive.

It has been thought that unregulated cell cycle progression may be a cause of malignant transformation of normal cells. On the other hand, inhibition of cell cycle progression through the S phase may cause replication error during DNA replication, which induces genomic instability and malignant transformation. Therefore, it is important to clarify the effect of HCV proteins on cell cycle progression in order to understand the molecular mechanism underlying the pathogenesis of HCV, including the development of HCC. A number of previous reports suggested that four HCV proteins—the core, NS3, NS4B, and NS5A—are involved in modulating cell cycle progression (Arima et al., 2001; Kato, 2001; Ray and Ray, 2001; Reed and Rice, 2000). For instance, the core protein promotes cell proliferation through the Ras/Raf signaling pathway and the anti-apoptotic function (Mar-

* Corresponding author. Fax: +81 86 235 7392.
E-mail address: nkato@md.okayama-u.ac.jp (N. Kato).
[1] Both authors contributed equally to this work.

0042-6822/$ - see front matter © 2005 Elsevier Inc. All rights reserved.
doi:10.1016/j.virol.2005.10.023

usawa et al., 1999; Tsuchihara et al., 1999). However, the core has been described to both enhance and repress the function of $p21^{Waf1/Cip1/Sdi1}$, a Cdk inhibitor (Dubourdeau et al., 2002; Jung et al., 2001; Lu et al., 1999; Ray et al., 1998). Recently, Scholle et al. found no significant cell cycle delay in human hepatoma HuH-7-based HCV RNA-replicating cells that were autonomously replicating genome-length HCV RNA, in comparison with cured cells of the same line from which HCV RNA had been eliminated by treatment with interferon (IFN)-α (Scholle et al., 2004). Hence, the effects of cell cycle regulation by HCV proteins are still controversial. Cancerous cell lines, such as the human hepatoma HuH-7 cell line (Hsu et al., 1993), which harbors a mutant *p53* gene, may not be suitable for addressing the effects of HCV proteins on cell cycle progression.

The PH5CH8 cell line was established by immortalization using the SV40 large-T antigen from non-neoplastic liver tissue of an HCV-related HCC patient (Ikeda et al., 1998; Noguchi and Hirohashi, 1996). PH5CH8 cells possess wild-type *p53* and *Rb* tumor suppressor genes. In nude mice, these cells reveal a non-malignant phenotype upon colony formation and tumorigenicity (Noguchi and Hirohashi, 1996), although the SV40 large-T antigen would partially repress the function of p53. Therefore, the PH5CH8 cell line is considered to be more relevant for studying the role of HCV proteins during hepatocarcinogenesis. We have previously reported that the HCV core protein activates the IFN-inducible 2′–5′-oligoadenylate synthetase gene in PH5CH8 cells (Naganuma et al., 2000). Recently, we demonstrated that the core protein's activation of this gene was mediated through the IFN-stimulated response element (ISRE) (Dansako et al., 2003). Furthermore, we found that the core protein promoted microsatellite instability in PH5CH8 cells (Naganuma et al., 2004). In fact, microsatellite instability was detected in approximately 20% of the tumor tissues from HCC patients examined, whereas no microsatellite instability was detected in normal liver tissues from the same patients (Dore et al., 2001; Kondo et al., 2000). In order to clarify the effect of HCV proteins on cell cycle progression in PH5CH8 cells, we examined cell cycle progression after the cells were released from the G1/S boundary in PH5CH8 cells expressing HCV proteins. We found that NS5B delays cell cycle progression by inducing IFN-β through the activation of the Toll-like receptor 3 (TLR3) signaling pathway without replicating viral genomes.

Results

HCV NS5B causes the delay of S phase progression

In a previous study of virus–host interactions, we examined whether or not HCV proteins affect cell cycle progression in PH5CH8 cells that stably expressed core or NS proteins. PH5CH8 cells were infected with retrovirus pCXbsr as a negative control (Ctr) or pCXbsr encoding either an HCV structural protein (HA-core) or NS protein (NS3, HA-NS4B, HA-NS5A, HA-NS5B, or NS5B), and we obtained PH5CH8 cells stably expressing each HCV protein. The expression of each HCV protein was confirmed by Western blot analysis (Fig. 1A). Then, the HCV protein-expressing cells were synchronized at the G1/S boundary, and cell cycle progression (from the S phase to the G2-M phase, then turning back to the G1 phase) was analyzed after the cells were released from synchronization. This cell cycle analysis revealed no significant differences in cell cycle progression between cells (PH/Ctr) infected with a control pCXbsr retrovirus and cells expressing core, NS3, NS4B, or NS5A (Fig. 1B). Unlike the PH/Ctr cells, the apparent delay of S phase progression was found in cells (PH/NS5B) expressing NS5B, regardless of the presence of the HA tag (Fig. 1B). To exclude the possibility that pCXbsr-derived retrovirus proteins synergistically affect the cell cycle together with NS5B, the retrovirus pCX4bsr vector (Akagi et al., 2003), which eliminates the production of any fusion proteins resulting from initiation at upstream AUG codons within the *gag* region of the vector, was used for the cell cycle analysis. As a result, the delay of S phase progression was found again in PH5CH8 cells expressing NS5B (Figs. 1A and C), suggesting that the retrovirus proteins are not involved in the delay of S phase progression. BrdUrd incorporation analysis was also carried out using PH/Ctr and PH/NS5B cells (Fig. 1D). In the PH/Ctr cells, DNA synthesis began early in the S phase (4 h after release). In the late S phase (8 h), more than 61% of the cells indicated final DNA synthesis. Thereafter, the cells either finished DNA replication in the G2-M phase (12 h) or returned to the G1 phase. In contrast, we found that DNA replication in most PH/NS5B cells predominantly remained in the early or middle S phase (8 h), and 49% of the cells were prolonged in the late S phase (12 h). To quantitatively evaluate this delay in S phase progression, the cells that had finished DNA replication were accumulated during the G2 phase by treatment with Nocodazole (Noc), which inhibits the progression of the G2 to M phases, after the cells were released from the G1/S transition. Whereas 77% of PH/Ctr cells reached the G2-M phase, only 37% of PH/NS5B cells did so (Fig. 1D). This level of decrease in cell numbers in the G2-M phase was not observed in PH5CH8 cells expressing core, NS3, NS4B, or NS5A (Fig. 1E), suggesting that NS5B specifically causes the delay of S phase progression in PH5CH8 cells. We further observed that the growth rate of PH/NS5B cells was significantly decreased relative to PH/Ctr cells (Fig. 1F), although the cell cycle distribution in asynchronous PH/NS5B cells was almost the same as that in asynchronous PH/Ctr cells (Fig. 1D). These results indicated that NS5B might delay the cell cycle progression of PH5CH8 cells in the S phase.

Cell cycle delay by NS5B is also found in other immortalized human hepatocytes

To clarify whether or not the delay of S phase progression by NS5B occurs in other human cell lines, we prepared three cell lines (Fig. 2A) that stably express NS5B–non-neoplastic human hepatocyte NKNT-3 (Kobayashi et al., 2000), hepatoma

HuH-7, and cervical carcinoma HeLa–and subjected them to the cell cycle analysis described above. The results revealed that S phase progression was delayed in NKNT-3, but not in HuH-7 or HeLa cells (Fig. 2B). This indicates that the delay of the cell cycle by NS5B expression is not limited to PH5CH8 cells.

IFN-β mediates the delay of S phase progression by NS5B

Since it has been reported previously that IFN-β induced the delay of S phase progression in human cultured cells (Vannucchi et al., 2000), we speculated that IFN-β was

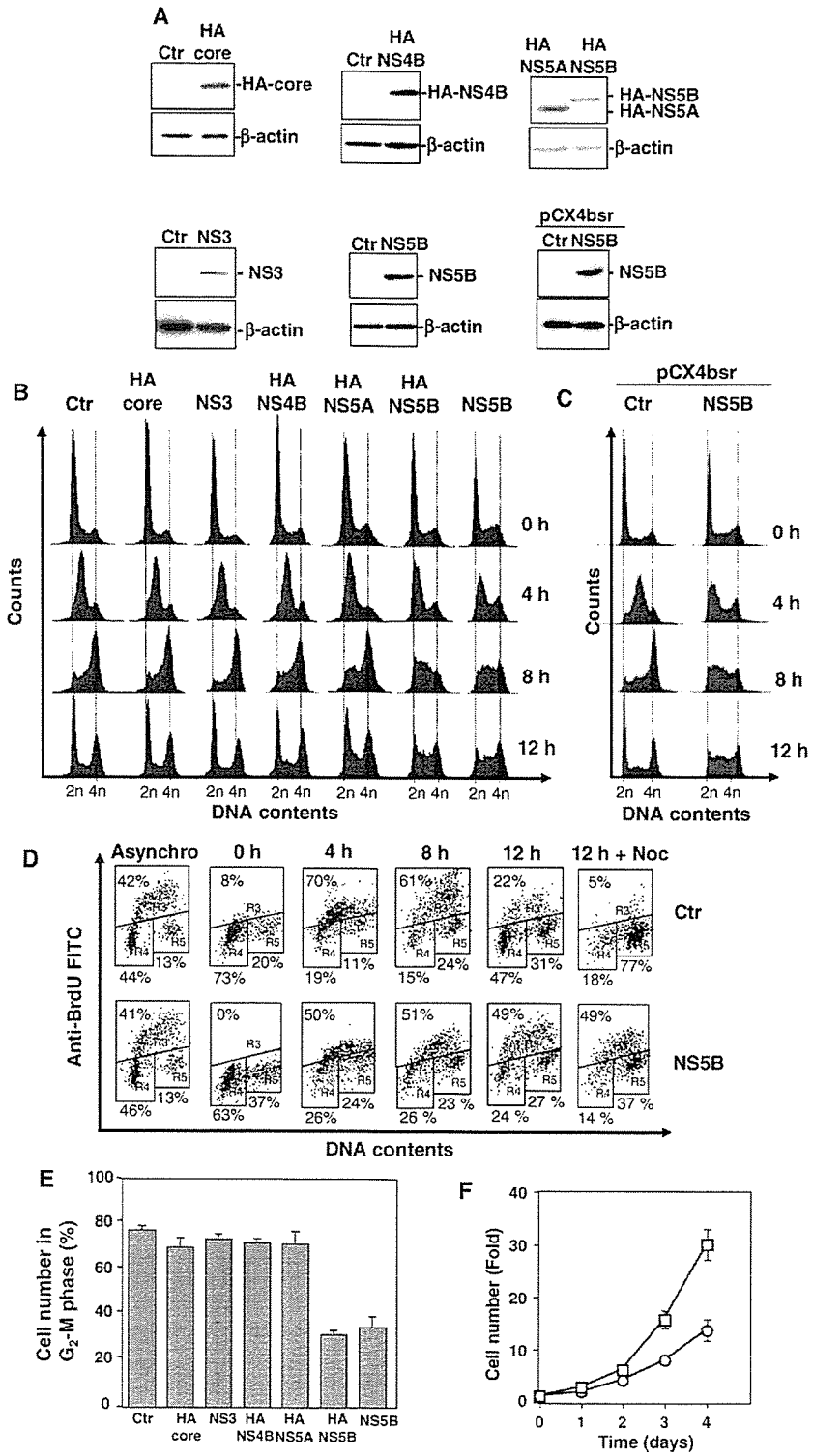

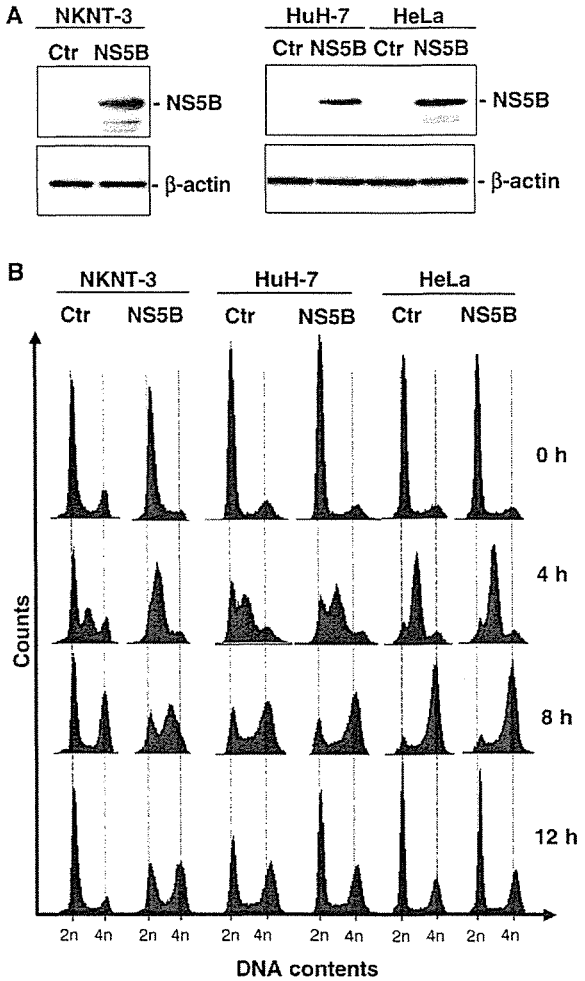

Fig. 2. NS5B delays S phase progression in another immortalized human hepatocytes. (A) Western blot analysis of NKNT-3, HuH-7, and HeLa cells infected with pCXbsr retrovirus encoding NS5B. The pCXbsr retrovirus was used as a control infection (Ctr). Anti-NS5B and anti-β-actin antibodies were used for the immunoblotting analysis. (B) Cell cycle analysis of NKNT-3, HuH-7, and HeLa cells expressing NS5B. NKNT-3, HuH-7, and HeLa cells that expressed NS5B (NS5B series) were synchronized, and cell cycle progression was analyzed as indicated in Fig. 1B. NKNT-3, HuH-7, and HeLa cells that were infected with the pCXbsr retrovirus were also analyzed as a control (Ctr series).

induced by NS5B. To evaluate this hypothesis, we examined whether or not PH/NS5B and NKNT-3 cells expressing NS5B (NK/NS5B) induce the expression of IFN-β. RT-PCR analysis clearly indicated that they did, and, at the same time, we found that HuH-7 and HeLa cells did not, despite their expression of NS5B (Fig. 3A). We next examined whether or not S phase progression is delayed in PH5CH8 and NKNT-3 cells treated with IFN-β prior to release from the G1/S boundary. As we expected, the S phase progression was stalled in PH5CH8 and NKNT-3 cells treated with IFN-β (Fig. 3B). We also observed that IFN-γ did not possess this activity of IFN-β (data not shown). These results suggest that the induction of IFN-β is implicated in the cell cycle delay in two immortalized human hepatocyte cell lines, PH5CH8 and NKNT-3.

To confirm the effect of IFN-β on cell cycle delay, we further examined whether or not treatment with anti-IFN-β neutralizing antibody can restore the cell cycle delay in PH/NS5B cells. The results showed that this treatment canceled the delay of S phase progression in PH/NS5B cells (Fig. 4A). BrdUrd incorporation analysis also showed that the proportion of cells reaching the G2-M phase was increased by the treatment with anti-IFN-β antibody in PH/NS5B cells (Fig 4B). These observations indicated that the expression of IFN-β mediated cell cycle delay during the S phase in PH/NS5B cells and suggested that the expression of NS5B induced IFN-β in PH5CH8 and NKNT-3 cells even without replication of the viral genome.

Activation of TLR3 signaling pathway by NS5B

Since IFN-β is known as a major cytokine induced by the activation of the TLR3 and TLR4 signaling pathways (Takeda et al., 2003), we next focused on which TLR pathway was activated for the production of IFN-β in PH/NS5B cells. To answer this question, TLR3- and TLR4-specific siRNAs were used to knock down TLR3 and TLR4 expression in PH/NS5B cells. TLR3 and TLR4 mRNAs were drastically decreased in PH/NS5B cells transfected with TLR3 and TLR4 siRNAs, respectively, but not in PH/NS5B cells transfected with GL2 siRNA (Elbashir et al., 2001) used as a control (Fig. 5A). This result indicates that the siRNAs used specifically contribute well to the degradation of TLR3 and TLR4 mRNAs. In this condition, IFN-β mRNA was significantly decreased in only PH/NS5B cells transfected with TLR3 siRNA (Fig. 5A), indicating that IFN-β expression in PH/NS5B cells is mediated through the TLR3 signaling pathway. The growth rate of PH/NS5B cells transfected with TLR3 siRNA was also accelerated, although TLR4 siRNA showed a rather lethal effect (Fig. 5B).

Fig. 1. HCV NS5B causes the delay of S phase progression. (A) Expression of HCV proteins in human cells introduced by retrovirus-mediated gene transfer. Western blot analysis of PH5CH8 cells infected with pCXbsr retroviruses encoding HCV proteins (HA-core, NS3, HA-NS4B, HA-NS5A, HA-NS5B, and NS5B) or pCX4bsr retrovirus encoding NS5B. pCXbsr or pCX4bsr retrovirus was used as a control infection (Ctr). Anti-HA (3F10, Roche), anti-NS3 (Novacastra), anti-NS5B, and anti-β-actin (Sigma) antibodies were used for the immunoblotting analysis. (B) Cell cycle analysis of PH5CH8 cells expressing HCV proteins. PH5CH8 cells that expressed HA-core, NS3, HA-NS4B, HA-NS5A, HA-NS5B, or NS5B were synchronized at G1/S boundary, and then cell cycle progression was monitored by flow cytometry after the release of the cells into the S phase at the indicated times. PH/Ctr cells that were infected with pCXbsr retrovirus were also analyzed as a control. (C) Cell cycle analysis of PH5CH8 cells infected with pCX4bsr retrovirus encoding NS5B. The cell cycle analysis was performed as described in panel B. (D) BrdUrd incorporation analysis of PH/Ctr and PH/NS5B cells. Cell cycle distribution of dot-plots of BrdUrd fluorescence versus DNA contents was analyzed in asynchronous or synchronized PH/Ctr and PH/NS5B cells. To measure the cells reaching the G2-M phase at 12 h after release, the cells were accumulated by Noc treatment. (E) Analysis of the cells reaching the G2-M phase. The percentage of cells at that phase was assessed by Noc treatment as indicated in panel D. The data are means ± SD of values from three independent experiments. (F) Growth curve of PH/Ctr and PH/NS5B cells. PH/Ctr (squares) or PH/NS5B (circles) were plated onto 6-well plates (3×10^4 cells per well), and the kinetics of cell proliferation during 4 days in culture were determined by trypan blue treatment. The data indicate average values ± SD from three independent experiments.

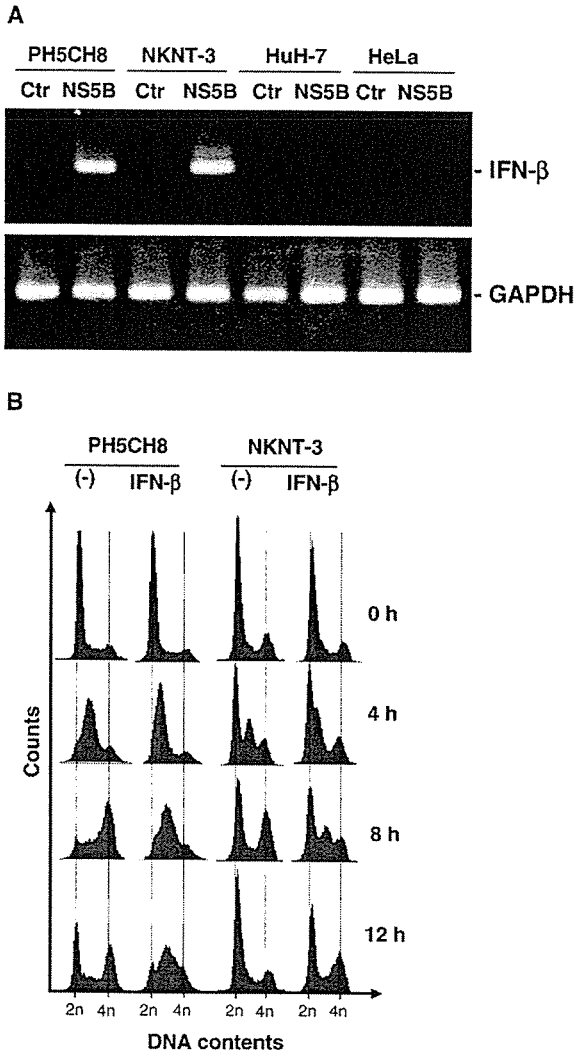

Fig. 3. IFN-β mediates the delay of S phase progression by NS5B. (A) RT-PCR analysis of IFN-β mRNA. The total RNAs were extracted from PH5CH8, NKNT-3, HuH-7, and HeLa cells (Ctr and NS5B series) and were subjected to RT-PCR analysis using primer sets for IFN-β (341 bp) and GAPDH (587 bp). (B) Cell cycle analysis of PH5CH8 and NKNT-3 cells treated with or without IFN-β. PH5CH8 and NKNT-3 cells were treated with or without IFN-β (500 IU/ml) at 12 h prior to release, and cell cycle progression was analyzed as indicated in Fig. 1B.

Furthermore, BrdUrd incorporation analysis using the Noc treatment revealed that 56% of PH/NS5B cells transfected with TLR3 siRNA reached the G2-M phase at 12 h after release, while only 33% of PH/NS5B cells transfected with GL2 siRNA reached that phase (Fig. 5C). The percentage of G2-M phase cells at 12 h after release was also 34% in PH/NS5B cells transfected with TLR4 siRNA, although the growth rate of these cells was lower than that of cells transfected with GL2 siRNA. These results indicated that the induction of IFN-β by NS5B expression was mediated through the activation of the TLR3 signaling pathway. This, in turn, demonstrated that TLR3 siRNA could override the delay of S phase progression in PH/NS5B cells.

To obtain further evidence that the induction of IFN-β by NS5B is mediated through TLR3, we prepared human embryonic kidney (HEK) 293 cells stably expressing TLR3 derived from PH5CH8 cells since it has been reported that ectopic expression of TLR3 can reconstruct the TLR3 signaling pathway in HEK293 cells (Alexopoulou et al., 2001). First, HEK293 cells were infected with retrovirus pCXbsr encoding NS5B or pCXbsr as a negative control (Ctr), yielding HEK293 cells (HEK/NS5B) stably expressing NS5B and control HEK293 cells (HEK/Ctr). Next, HEK/NS5B and HEK/Ctr cells were infected with

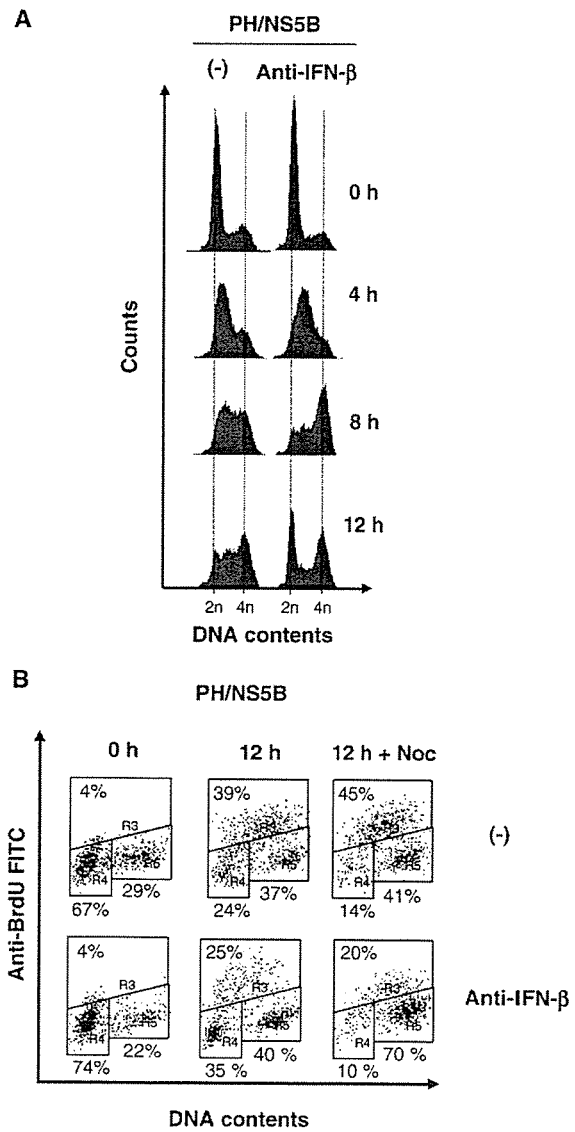

Fig. 4. Treatment with anti-IFN-β antibody canceled the delay of S phase progression. (A) Cell cycle analysis of PH/NS5B cells treated with or without anti-IFN-β antibody. PH/NS5B cells were treated with anti-IFN-β antibody (70 U/ml, Oxford Biotechnology) during cell cycle synchronization and after release from the G1/S boundary. (B) BrdUrd incorporation analysis of PH/NS5B cells treated with or without anti-IFN-β antibody. The antibody was used as indicated in panel A. Noc was used as indicated in Fig. 1D.

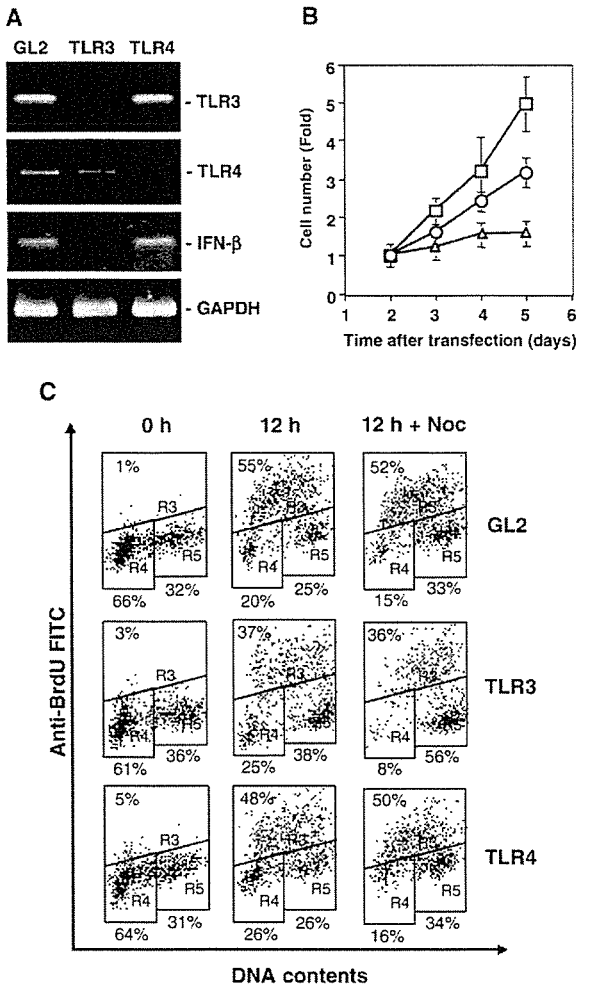

Fig. 5. Activation of IFN-β gene by NS5B is mediated through the TLR3 signaling pathway. (A) Down-regulation of IFN-β mRNA by transfection of TLR3 siRNA. PH/NS5B cells were transfected with dsRNA duplexes targeting TLR3, TLR4, or luciferase GL2. After 3 days, the expression levels of TLR3, TLR4, IFN-β, and GAPDH mRNAs were examined by RT-PCR. (B) Growth curve of PH/NS5B cells transfected with siRNAs. After 2 days of transfection, the proliferation kinetics of PH/NS5B cells transfected with GL2 (circles), TLR3 (squares), and TLR4 (triangles) siRNAs were analyzed as indicated in Fig. 1F. (C) BrdUrd incorporation analysis of PH/NS5B cells transfected with GL2, TLR3, and TLR4 siRNAs. After 2 days of transfection, the cells were synchronized, and cell cycle progression was analyzed as indicated in Fig. 1D.

retrovirus pCXpur encoding TLR3 or pCXpur as a negative control, yielding cells stably expressing TLR3 and control HEK293 cells. The expression of NS5B or TLR3 was confirmed by Western blot analysis (Fig. 6A). We then performed a dual-luciferase reporter assay using an IFN-β gene promoter. The results revealed that the luciferase activity was enhanced in only the HEK293 cells stably expressing both NS5B and TLR3 (Fig. 6B). This suggests that TLR3 mediates NS5B's induction of IFN-β. However, since the enhancement of luciferase activity was approximately two-fold, we failed to detect the enhancement of the mRNA expression levels for IFN-β and one of its target genes, ISG56 (data not shown). To accurately assess the enhancement, high expression levels of NS5B and TLR3 in HEK293 cells will be needed.

The RIG-I-mediated signaling pathway is not implicated in the induction of IFN-β in PH/NS5B cells

Recently, RIG-I, a cellular DExD/H box helicase, was found to be a double-stranded RNA (dsRNA) binding protein that functions independently of TLR3 to induce IFN-β in response to viral infection (Yoneyama et al., 2004). Since another recent study showed that both the TLR3- and RIG-I-mediated signaling pathways are functional in PH5CH8 cells (Li et al., 2005a, 2005b), we examined whether or not the RIG-I-mediated signaling pathway is involved in NS5B's induction of IFN-β. First, PH/NS5B and PH/Ctr cells were infected with retrovirus pCXpur encoding myc-tagged RIG-IC, a dominant negative inhibitor of RIG-I harboring only the helicase domain but not the two N-terminal CARD domains (Yoneyama et al., 2004), or pCXpur as a negative control. Cells that stably expressed myc-tagged RIG-IC were thus obtained. The expression of myc-

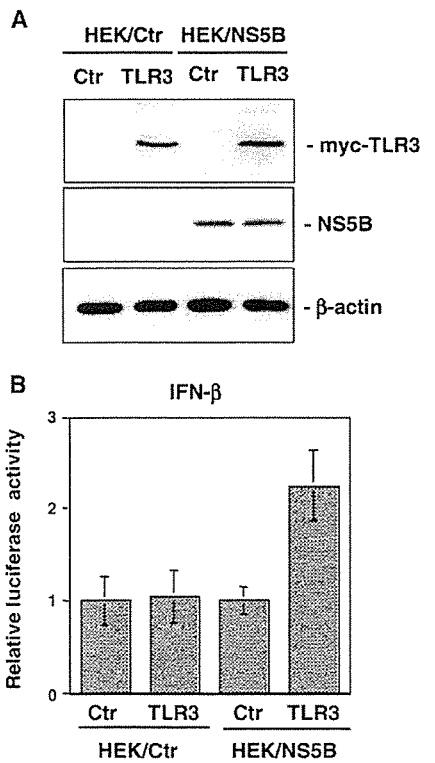

Fig. 6. Ectopic expression of TLR3 enhances the IFN-β gene promoter in only the HEK293 cells stably expressing NS5B. (A) Expression of TLR3 and NS5B in HEK293 cells introduced by retrovirus-mediated gene transfer. Western blot analysis of HEK/Ctr or HEK/NS5B cells infected with pCXpur retrovirus encoding myc-tagged TLR3 was performed. The pCXpur retrovirus was used as a control infection. Anti-myc, anti-NS5B, and anti-β-actin antibodies were used for the immunoblotting analysis. (B) Dual luciferase reporter assay of the IFN-β gene promoter. The cells shown in panel A were transfected with pIFN-β(-125)-Luc, and the dual luciferase assay was performed as described previously (Dansako et al., 2003). Data are means ± SD from three independent triplicate experiments.

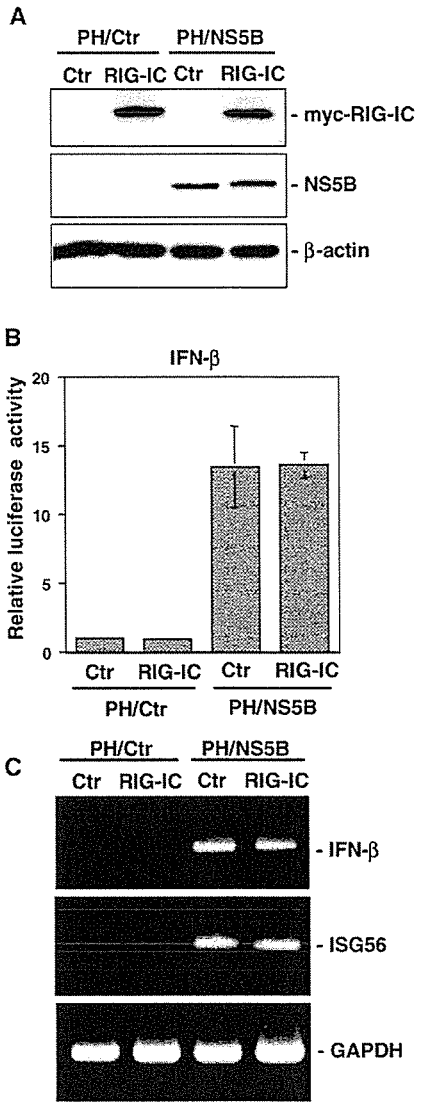

Fig. 7. Induction of IFN-β by NS5B is not mediated through the RIG-I signaling pathway. (A) Expression of RIG-IC and NS5B in PH5CH8 cells introduced by retrovirus-mediated gene transfer. Western blot analysis of PH/Ctr or PH/NS5B cells infected with pCXpur retrovirus encoding myc-tagged RIG-IC was performed. The pCXpur retrovirus was used as a control infection. Anti-myc, anti-NS5B, and anti-β-actin antibodies were used for the immunoblotting analysis. (B) Dual luciferase reporter assay of the IFN-β gene promoter. The cells shown in panel A were transfected with pIFN-β(-125)-Luc, and the dual luciferase assay was performed as indicated in Fig. 6B. (C) RT-PCR analysis of IFN-β and ISG56 mRNAs. The total RNAs were extracted from the cells shown in panel A and subjected to RT-PCR analysis using primer sets for IFN-β (341 bp), ISG56 (320 bp), and GAPDH (587 bp).

tagged RIG-IC was confirmed by Western blot analysis (Fig. 7A). Using PH/Ctr cells stably expressing myc-tagged RIG-IC, we confirmed that IFN-β production was markedly suppressed after infection with Sendai virus (data not shown), as initially observed in Newcastle disease virus infection (Yoneyama et al., 2004). This indicates that RIG-IC functions as a dominant negative inhibitor of RIG-I in PH5CH8 cells. We then performed a dual-luciferase reporter assay using an *IFN-β* gene promoter. The results revealed that the enhancement of luciferase activity in PH/NS5B cells was not suppressed regardless of RIG-IC expression (Fig. 7B). Furthermore, the mRNA expression levels for IFN-β and one of its target genes, ISG56, were also unchanged by the expression of RIG-IC (Fig. 7C). These results suggest that NS5B's induction of IFN-β is not mediated through the RIG-I signaling pathway.

NS5B does not interact with TLR3 adaptor protein

Since we showed that NS5B's induction of IFN-β was mediated through the TLR3 but not the RIG-I signaling pathway, we further examined the mechanism underlying IFN-β induction by testing the possibility of interaction between NS5B and the TLR3 adaptor protein TRIF (Yamamoto et al., 2002). We prepared HEK/NS5B cells stably expressing myc-tagged NS5A or myc-tagged TRIF and examined whether or not NS5B interacts with TRIF by an immunoprecipitation method following Western blot analysis. The results clearly showed that NS5B and myc-tagged NS5A were co-immunoprecipitated by anti-myc antibody as reported previously (Shirota et al., 2002). However, co-immunoprecipitation of NS5B and myc-tagged TRIF was clearly not observed (Fig. 8). This result suggests that the activation of the TLR3 signaling pathway by NS5B occurs through one or more factors other than TRIF.

Induction of IFN-β depends on RNA-dependent RNA polymerase (RdRp) activity of NS5B

Since dsRNA, an intermediate of viral replication, is known as a natural ligand for the activation of TLR3 (Alexopoulou et

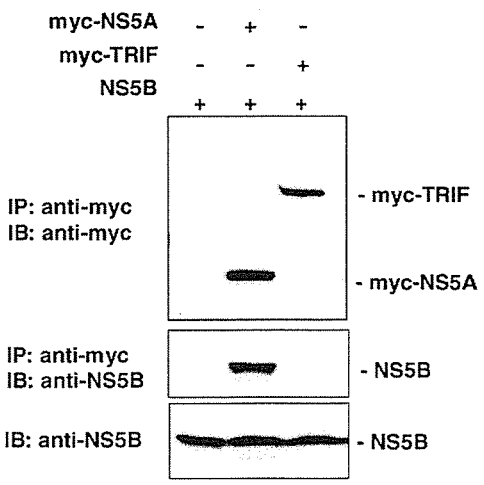

Fig. 8. NS5B does not interact with TRIF. HEK/NS5B cells were infected with pCXpur retrovirus encoding myc-tagged NS5A (middle lane) or myc-tagged TRIF (right lane). pCXpur retrovirus was used as a control infection (left lane). Cell lysate was immunoprecipitated (IP) with anti-myc antibody-conjugated agarose beads. The immunoprecipitates were resolved by SDS-PAGE, and anti-myc (upper panel) and anti-NS5B (middle panel) antibodies were used for the immunoblotting (IB) analysis. To confirm the expression level of NS5B, cell lysates were subjected to immunoblotting analysis using anti-NS5B antibody (lower panel).

al., 2001; Takeda et al., 2003), we next examined whether or not the induction of IFN-β in human hepatocytes expressing NS5B (591 amino acids; amino acids 2420 to 3010 in the HCV-1b genotype) (Kato et al., 1990) depends on NS5B's RdRp activity. Since this activity is already well characterized (Hagedorn et al., 2000), we constructed several NS5B mutants to evaluate this subject (Fig. 9A). One is the substitution mutant G2736V of the GDD motif (amino acids 2736–8) located in the catalytic site, and the other is the deletion mutant Δ2575–7 (R2753T, K2754S, and Δ2575–7) at the priming and interrogation sites, all of which are essential for NS5B's RdRp activity (Behrens et al., 1996; Bressanelli et al., 2002). We also constructed three carboxyl-truncated forms (ΔC21, ΔC56, and ΔC97, lacking 21, 56, and 97 amino acids, respectively) of NS5B. These truncated mutants of NS5B lack the last 21 hydrophobic amino acids, which are necessary and sufficient to target NS5B to the cytosolic side of the endoplasmic reticulum (ER) membrane (Schmidt-Mende et al., 2001; Yamashita et al., 1998). Although ΔC21 and ΔC56, but not ΔC97, possess RdRp activity in vitro, ΔC56 shows higher RdRp activity than ΔC21 because only the latter possesses a regulatory motif inhibiting RNA binding and polymerase activity (Leveque et al., 2003). We prepared PH5CH8 cells stably expressing these NS5B mutants and then performed cell cycle analysis using these

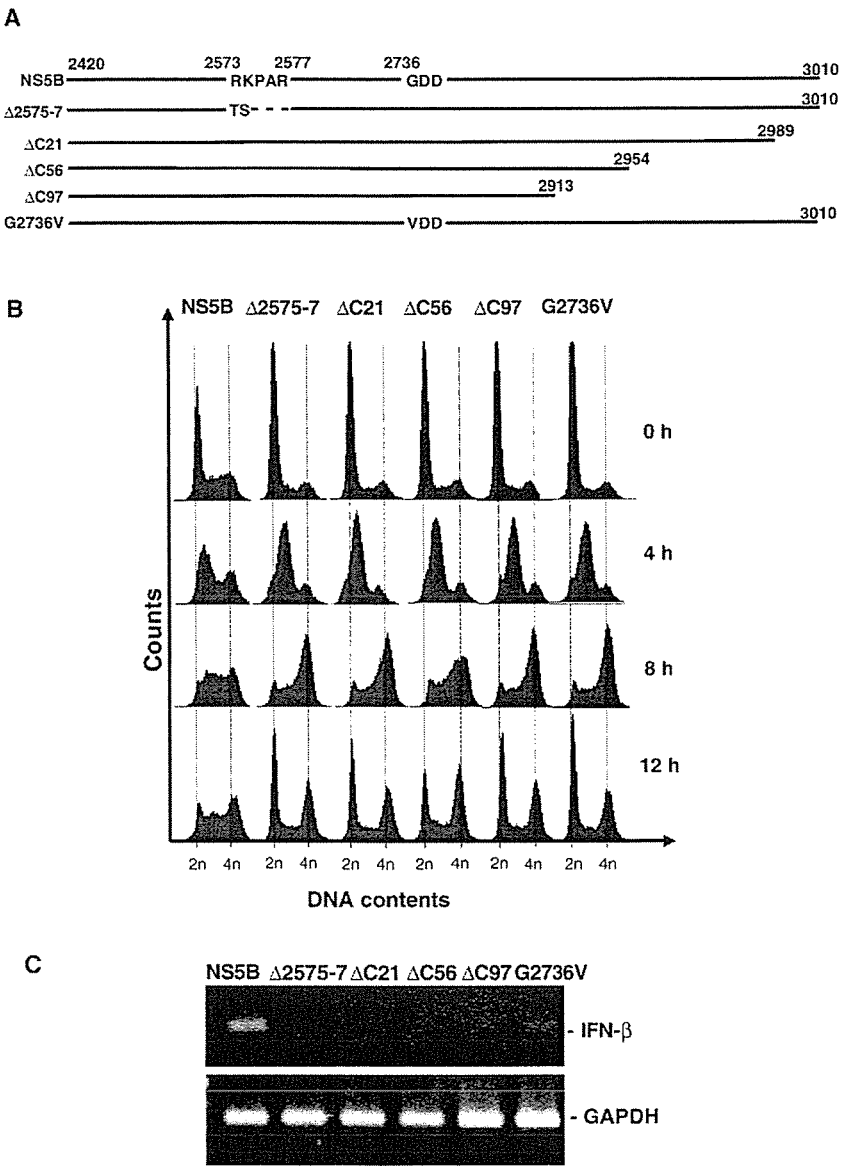

Fig. 9. The RdRp activity of NS5B anchoring on ER membrane is required for induction of IFN-β and following the delay of S phase progression. (A) Schematic presentation of the NS5B mutants used. Only amino acid sequences in the mutated regions of NS5B are indicated. (B) Cell cycle analysis of PH/NS5B and PH5CH8 cells expressing NS5B mutants. Cell cycle distribution was analyzed as described in Fig. 1B. (C) RT-PCR analysis of IFN-β mRNA in PH/NS5B and PH5CH8 cells expressing NS5B mutants. RT-PCR analysis was performed as described in Fig. 3A.

prepared cells. The results revealed no effect on S phase progression in the PH5CH8 cells expressing NS5B mutants (Fig. 9B), although PH5CH8 cells expressing ΔC56 showed a slight delay of S phase progression. Induction of IFN-β mRNA was also not observed in the PH5CH8 cells expressing NS5B mutants (Fig. 9C). These results revealed that the delay of S phase progression and the induction of IFN-β depend on the RdRp activity of NS5B, and these effects are coupled with ER membrane anchorage of NS5B in cells.

To examine the activation of IRF3, a factor specifically induced by stimulated TLR3 or TLR4, by the expression of NS5B and its mutants, we performed a dual-luciferase reporter assay using a synthetic promoter having five repeats of the consensus ISRE, which was the same as the IRF3 target sequence in the *IFN-β* gene promoter (Fig. 10A) and an intrinsic *IFN-β* gene promoter (Fig. 10B). The results showed that the luciferase activity was enhanced approximately five-fold (Fig. 10A) and eight-fold (Fig. 10B) only in PH/NS5B cells,

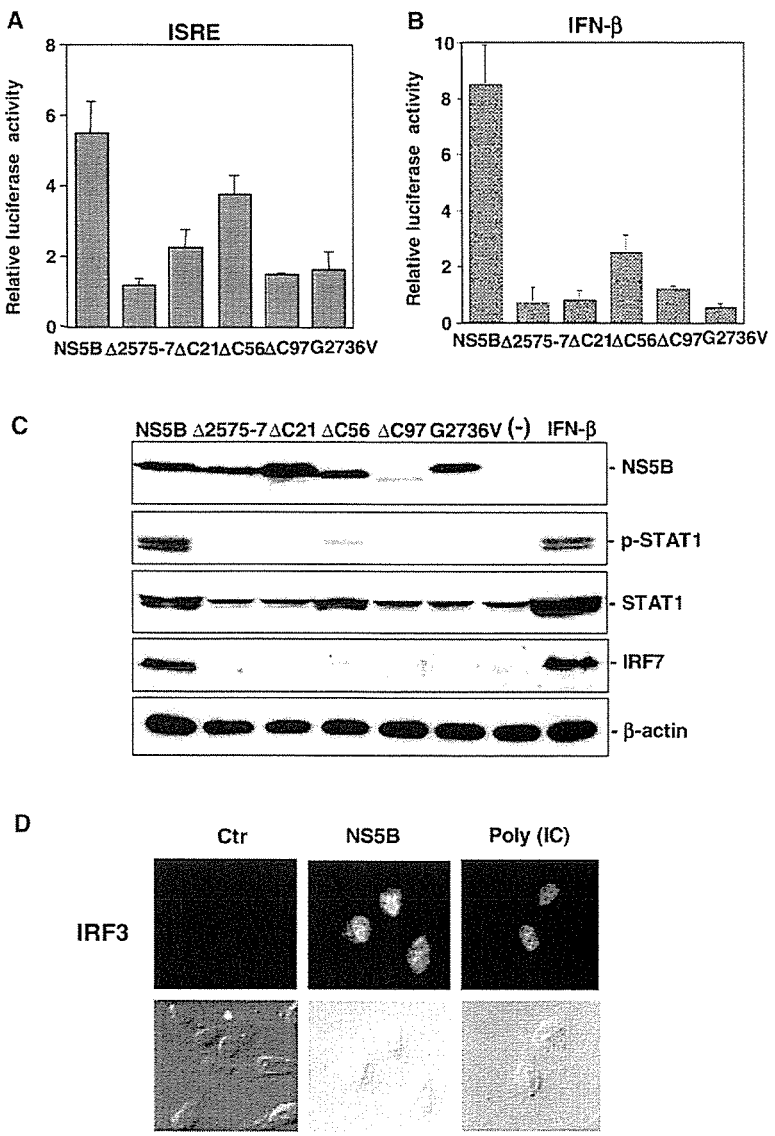

Fig. 10. NS5B full form is required for activation of IRF3 target sequences and IFN-β signaling pathway. (A) Dual luciferase reporter assay toward IRF3 target sequences. PH5CH8 cells were transfected with the pISRE-Luc (Stratagene) and pCXbsr encoding NS5B or its mutant, and the dual luciferase assay was performed as indicated in Fig. 6B. The lysates of cells transfected with pCXbsr were used as a control. (B) Dual luciferase reporter assay of the IFN-β gene promoter. Dual luciferase assay was performed as described in panel A except using pIFN-β(-125)-Luc instead of pISRE-Luc. (C) Western blot analysis of the components involved in the IFN-β signaling pathway. The lysates of PH/NS5B and PH5CH8 cells expressing NS5B mutants were subjected to immunoblotting using anti-NS5B, anti-p-STAT1(Y701), anti-STAT1, anti-IRF7, and anti-β-actin antibodies. PH5CH8 cells treated with or without IFN-β (500 IU/ml for 24 h) were also analyzed as a control. (D) Subcellular distribution of endogenous IRF3. PH/Ctr and PH/NS5B cells were processed and stained with anti-IRF3 antibody and an FITC-conjugated secondary antibody. PH5CH8 cells treated with poly (IC) were also used as a positive control.

suggesting that IRF3 is activated by the NS5B full form. Interestingly, however, luciferase activity was enhanced approximately four-fold (Fig. 10A) and three-fold (Fig. 10B) in PH5CH8 cells expressing ΔC56, although the enhancement was not as great as the five-fold (Fig. 10A) and eight-fold (Fig. 10B) in PH/NS5B cells, respectively. We then examined the phosphorylation status of STAT1 on Y701 and the level of IRF7, one of the downstream targets of the IFN-β signaling pathway (Katze et al., 2002). Western blot analysis revealed marked phosphorylation of STAT1 and IRF7 expression in PH/NS5B cells as well as in PH5CH8 cells treated with IFN-β (Fig. 10C). Although slight phosphorylation of STAT1 was observed in the PH5CH8 cells expressing ΔC56, IRF7 expression was not observed (Fig. 10C). Unlike PH/NS5B cells and PH5CH8 cells expressing ΔC56, neither the phosphorylation of STAT1 nor the expression of IRF7 was detected in PH5CH8 cells expressing other NS5B mutants. These results indicated that ΔC56 had an extremely low ability to induce IFN-β after activation of TLR3, although ΔC56 was still able to enhance the IRF3 target promoter. To obtain further evidence of the activation of IRF3, we examined the subcellular distribution of endogenous IRF3 in PH/Ctr and PH/NS5B

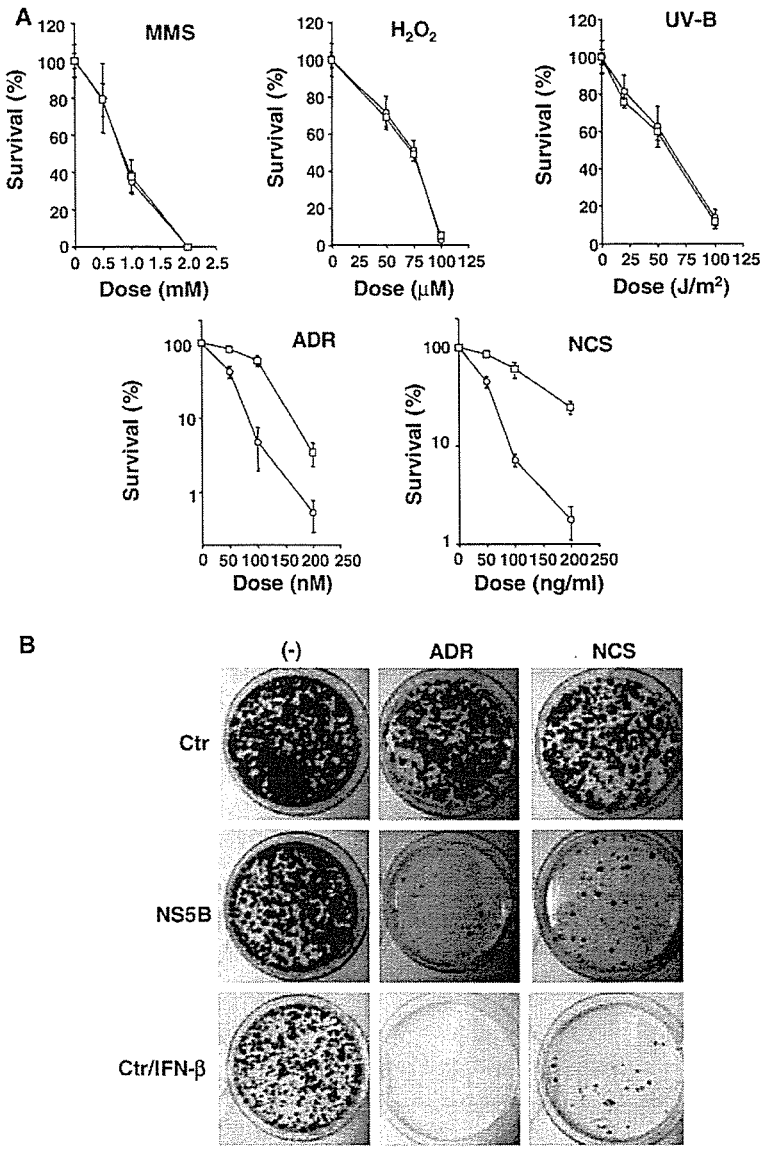

Fig. 11. Sensitivity of PH/NS5B cells against DNA-damaging reagents. (A) Clonogenic assays for PH/Ctr (square) and PH/NS5B (circle) cells after treatment with increasing doses of DNA-damaging reagents. Cells were treated with MMS, H_2O_2, UV-B, ADR, and NCS. Ten days after the treatment, cells were fixed and stained with Coomassie brilliant blue. Only colonies containing >50 cells were scored as being derived from viable clonogenic cells. Data are means ± SD from two independent triplicate experiments. (B) PH/Ctr, PH/NS5B, and IFN-β-treated (20 IU/ml) PH/Ctr cells were treated with ADR (100 nM) or NCS (100 ng/ml). The panels show survived colonies that are stained with Coomassie brilliant blue at 10 days after the treatment.

cells. In PH/Ctr cells, IRF3 was distributed in a perinuclear and/or cytoplasmic context. However, in PH/NS5B cells as well as PH5CH8 cells treated with poly (IC), IRF3 was distributed to the nucleus, a finding consistent with its activated state (Fig. 10D). Taken together, our findings indicate that the RdRp activity of HCV NS5B anchoring on ER membrane is necessary and sufficient to activate the TLR3 signaling pathway.

PH/NS5B cells are more susceptible than PH/Ctr cells to DNA-damaging reagents

To better understand the effect of IFN-β induction in PH/NS5B cells, we next examined the susceptibilities of PH/NS5B and PH/Ctr cells against various types of DNA-damaging reagents. A clonogenic assay using PH/NS5B and PH/Ctr cells was performed by treatment with MMS (a DNA alkylating reagent) and H_2O_2 (a DNA oxidative reagent) and by UV-B irradiation, which induces DNA single-strand breaks and/or thymidine dimer formation in DNA. ADR and NCS, which induce DNA double-strand breaks, were also used for the clonogenic assay. As shown in Fig. 11A, PH/NS5B and PH/Ctr cells were susceptible to the MMS treatment, the H_2O_2 treatment, and the UV-B irradiation, and no differences were observed between their susceptibilities. Interestingly, however, PH/NS5B cells were more susceptible than PH/Ctr cells against ADR or NCS treatment (Fig. 11A). These results suggest that PH/NS5B cells are more sensitive than PH/Ctr cells to damage in the form of DNA double-strand breaks. To clarify whether or not IFN-β induction increases the susceptibility against ADR or NCS treatment, we examined the effect of ADR or NCS in PH/Ctr cells treated with IFN-β. In this treatment, the cells changed to susceptible phenotype against ADR or NCS treatment, as observed in PH/NS5B cells (Fig. 11B). These results suggest that IFN-β induced by NS5B in PH5CH8 cells changes the cells into the hypersensitive phenotype, making them susceptible to DNA damage in the form of double-strand breaks.

Discussion

In the present study, we found that HCV NS5B induced IFN-β in two kinds of immortalized human hepatocyte cell lines, PH5CH8 and NKNT-3. We showed that NS5B's induction of IFN-β was mediated through the TLR3 but not the RIG-I signaling pathway. The induction of IFN-β caused the delay of cell cycle progression through the S phase in these cells. Since it has been generally known that the activation of the TLR3 signaling pathway is caused by dsRNA, a molecular pattern associated with replicating viral genomes, we first obtained data suggesting that dsRNA is generated by NS5B even without replication of the viral genome.

TLRs belong to a family of evolutionarily conserved innate immune recognition molecules, and ten members of the TLR family have been identified in human (Medzhitov, 2001; Takeda et al., 2003). TLR3 recognizes dsRNA and induces the antiviral immune responses (Alexopoulou et al., 2001; Matsumoto et al., 2002). TLR3 activates transcription factor IRF3 through TRIF, leading to IFN-β production (Oshiumi et al., 2003; Yamamoto et al., 2002, 2003). We speculated on two possible mechanisms underlying the activation of the TLR3 signaling pathway by NS5B. The first possibility is that protein–protein interaction between NS5B and TRIF is involved in the activation of the TLR3 signaling pathway. However, we failed to obtain evidence of direct interaction between NS5B and TRIF. The second possibility is that the RdRp activity of NS5B contributes to the activation of TLR3. To evaluate this hypothesis, we examined whether or not several NS5B mutants, including carboxyl-truncated mutants or an RdRp activity-defective mutant (G2736V), could induce IFN-β. The experimental data clearly showed that neither the G2736V mutant nor the carboxyl-truncated mutants could induce IFN-β. Therefore, we suggested that NS5B RdRp activity anchoring the ER membrane is critical for the activation of the TLR3 signaling pathway.

The finding that NS5B RdRp activity on the ER membrane was a critical factor for the induction of IFN-β surprised us because we expected that dsRNA, a natural ligand for TLR3, was produced in NS5B-expressing hepatocyte cells without replication of the viral RNA genome. Therefore, we now presume a daring hypothesis: that NS5B can produce dsRNA using cellular RNA as a template on the ER membrane. Since no direct evidence has been found to support this hypothesis at this stage, further experiments are necessary to evaluate this hypothesis. For instance, if possible, the detection of newly synthesized dsRNA in NS5B-expressing cells or the detection of newly synthesized dsRNA by recombinant NS5B using cellular RNA in vitro may become positive evidence. Furthermore, since the formation of a membrane-associated replication complex is a characteristic of positive-stranded RNA viruses, including HCV (Shi et al., 2003), it will also be interesting to examine whether or not the RdRps of the other RNA viruses possess novel activity similar to that observed in this study. At least we recently detected that NS5B derived from an HCV-2a genome designated JFH-1, which produces virus particles infectious for HuH-7 cells (Wakita et al., 2005), also strongly induced IFN-β in PH5CH8 cells (Ikeda et al., unpublished data). In addition, we are not able to completely exclude the possibility that NS5B-encoding RNA, but not NS5B, specifically activates the TLR3 signaling pathway. However, this possibility is unlikely because the G2736V mutant with only one nucleotide substitution could not activate the TLR3 signaling pathway.

Since the activation of the TLR3 signaling pathway in NS5B-expressing PH5CH8 or NKNT-3 cells is considered to be due to a novel function of NS5B, it is important to clarify whether or not this function occurs in the HCV life cycle. Although HCV replicon systems carrying autonomously replicating HCV RNA genomes developed using HuH-7 (Blight et al., 2000; Ikeda et al., 2002; Lohmann et al., 1999) and HeLa (Zhu et al., 2003) cells have become powerful tools for basic studies of HCV, these systems would not be suitable to prove our hypothesis because the induction of IFN-β by NS5B was not observed in HuH-7 or HeLa cells, in which the TLR3 signaling pathway was suggested to be defective. In fact, it has been recently reported that HuH-7 cells lack a TLR3